Constraints imposed by rift inheritance on the compressional reactivation of a hyperextended margin: mapping rift domains in the North Iberian margin and in the Cantabrian Mountains

P. Cadenas [(1)], G. Fernández-Viejo [(1)], J.A. Pulgar [(1)], J. Tugend [(2)], G. Manatschal [(2)] & T.A. Minshull [(3)]

(1): Department of Geology, University of Oviedo, Oviedo, Spain

(2): Institut du Physique du Globe de Strasbourg; UMR 7516, Université de Strasbourg/EOST, CNRS Strasbourg, France

(3): Ocean and Earth Science, National Oceanography Centre Southampton, University of Southampton, Southampton, United Kingdom

*corresponding author: pcadenas@geol.uniovi.es

Key Points

We define rift domains and their boundaries in the western and central North Iberian margin using geological and geophysical data.

The North Iberian margin shows structural variability resulting from polyphase rifting and subsequent compressional reactivation

Rift domains controlled the subsequent inversion conditioning the current structure of the North Iberian margin and the Cantabrian Mountains

Abstract

The Alpine Pyrenean-Cantabrian orogen developed along the plate boundary between Iberia and Europe, involving the inversion of Mesozoic hyperextended basins along the southern Biscay margin. Thus, this margin represents a natural laboratory to analyse the control of structural rift inheritance on the compressional reactivation of a continental margin. With the aim to identify former rift domains and investigate their role during the subsequent compression, we performed a structural analysis of the central and western North Iberian margin, based on the interpretation of seismic reflection profiles and local constraints from drill-hole data. Seismic interpretations and published seismic velocity models enabled the development of crustal thickness maps that helped to constrain further the offshore and onshore segmentation. Based on all these constraints, we present a rift domain map across the central and western North Iberian margin, as far as the adjacent western Cantabrian Mountains. Furthermore, we provide a first-order description of the margin segmentation resulting from its polyphase tectonic evolution. The most striking result is the presence of a hyperthinned domain (e.g. Asturian Basin) along the central continental platform that is bounded to the north by the Le Danois High, interpreted as a rift-related continental block separating two distinctive hyperextended domains. From the analysis of the rift domain map and the distribution of reactivation structures, we conclude that the landward limit of the necking domain and the hyperextended domains respectively guide and localize the compressional overprint. The Le Danois block acted as a local buttress, conditioning the inversion of the Asturian Basin.

Keywords: Bay of Biscay rift system, North Iberian margin, Cantabrian Mountains, hyperextension, underthrusting, segmentation.

1) Introduction

The understanding of the structure and evolution of rifted margins and of the processes involved in their formation and reactivation has improved remarkably over the past two decades. For instance, the concept of polyphase rifting including successive deformation modes that develop since the initiation of crustal stretching until the onset of oceanic accretion is now widely accepted [e.g., *Boillot* & *Froitzheim* 2001; *Lavier* & *Manatschal*, 2006]. Regardless of their variability, worldwide hyperextended rifted margins share a comparable large-scale organization into distinctive domains defined from different approaches and observations made at different scales [e.g., *Dean et al.*, 2000; *Lagabrielle et al.*, 2010; *Masini et al.*, 2013; *Mohn et al.*, 2012; *Pérez-Gussinyé et al.*, 2003; Péron-*Pinvidic et al.*, 2013; *Sutra et al.*, 2013]. In the case of magma-poor rifted margins, five structural domains can be distinguished which are referred to as: proximal, necking, hyperthinned, exhumed mantle and oceanic domains (Figure 1a) [*Tugend et al., 2015a*]. The hyperthinned and exhumed mantle domains are referred in some studies together as the distal [e.g. *Péron-Pinvidic et al.*, 2013] or hyperextended domain [*Mohn et al.*, 2015; this study].

The various rift domains are characterized by different structures, a particular sediment geometries and basement type (Figure 1a and b), suggesting that they result from different modes of deformation [*Sutra et al.*, 2013] that migrate progressively towards the area of the future breakup [*Péron-Pinvidic & Manatschal*, 2009]. Thus, defining and mapping the different rift domains along a rifted margin can improve the understanding of its formation and allow the comparison with lithospheric scale numerical models [e.g., *Lavier* & *Manatschal*, 2006; *Huismans & Beaumont*, 2011; *Brune et al.*, 2014]. Rift domains also have different rheological profiles, which will influence any subsequent reactivation of the continental margin [*Péron-Pinvidic et al.*, 2008; *Tugend et al.*, 2014]. In reactivated magma-poor rifted margins, the mapping of rift domains can provide important constraints about the rift architecture [*Tugend et al.*, 2014], thus facilitating quantitative restoration of hyperextended domains [*Sutra et al.*, 2013] in the absence of well-constrained magnetic anomalies [e.g., *Nirrengarten et al.*, 2017]. Furthermore, palinspatic restorations of collisional mountain belts often do not consider the early stages of convergence, that are frequently erased during the later deformation stages. This omission results in underestimation of the initial shortening [*Mouthereau et al.*, 2014] undergone by the hyperthinned and exhumed mantle domains. However, the identification of early reactivation of hyperextended domains may be crucial to explain some of the current features of Alpine type collisional mountain belts. In this sense, the Bay of Biscay is a remarkable setting preserving early stages of inversion. The mapping of rift domains on this area is also useful to constrain regional Iberian plate kinematic reconstructions, where the disputed nature of the M-series magnetic anomalies [*Nirrengarten et al*., 2017] has led to different plate kinematic scenarios [*Barnett-Moore et al.*, 2016].

Marking the southern Bay of Biscay, the North Iberian margin corresponds to a strongly segmented, partially inverted, hyperextended magma-poor rifted margin [*Derégnaucourt & Boillot*, 1982*; Roca et al.*, 2011;

Tugend et al., 2014]. In this work, we focus notably on the central and western North Iberian margin, including the Asturian Basin and the Le Danois High. *Tugend et al.* [2014, 2015b], who developed a rift domain map for the entire Bay of Biscay-Pyrenean system, included this area as part of a wide necking domain. Previous authors linked the strong segmentation observed within the rift system to the presence of transfer zones, such as the Santander Transfer zone offshore [*Roca et al.*, 2011], and continental blocks such as the Landes High [*Ferrer et al.*, 2008; *Tugend et al.*, 2014]. In the abyssal plain, the oceanic crust recognized in the western corner evolves to a transitional basement towards the east [*Álvarez-Marrón et al.*, 1996; *Fernández-Viejo et al.*, 1998; *Ruiz*, 2007]. *Roca et al.* [2011] and *Tugend et al.* [2014, 2015b] interpreted on this area extremely thinned continental crust and former exhumed mantle. The anomalous mantle velocities recognized beneath the continental platform have been attributed to serpentinized exhumed mantle now underthrust beneath the margin due to the Alpine inversion [*Fernández-Viejo et al.*, 2012; *Roca et al.*, 2011]. The margin underwent a compressional reactivation varying between mild inversion and crustal wedging [*Álvarez-Marrón et al.*, 1997; *Fernández-Viejo et al.*, 2011; *Gallastegui et al.*, 2002*; Roca et al.*, 2011]. The central and western North Iberian margin are now incorporated, together with the Cantabrian Mountains, into the Pyrenean-Cantabrian collisional chain [*Fernández-Viejo et al.*, 2000; *Pulgar et al.*, 1996] making this area a unique natural laboratory to study and analyse the influence of rift inheritance on the inversion of a hyperextended rifted margin.

Using a dense set of new high quality 2D seismic reflection data and boreholes, combined with a synthesis of published results from wide-angle seismic data (Figure 2) we present a detailed map of the rift domains focused on the central and western North Iberian margin and also including the onshore western Cantabrian Mountains. Our work builds on the method developed and applied by *Tugend et al.* [2014, 2015b]. Based on this more detailed mapping, we aim to constrain further, how rift architecture conditioned the subsequent compressional reactivation that led to the development of the present-day structure. Moreover, we add some more insights to comprehend the margin segmentation resulting from polyphase rifting and the subsequent compressional reactivation.

2) Tectonic Setting

The structure of the North Iberian margin resulted from successive tectonic events linked to the complex palaeographic evolution of the Iberian domain since the Permian. This margin developed during polyphase Triassic to Lower Cretaceous transtensional and extensional rift events and was subsequently reactivated during Alpine orogeny [e.g., *Boillot et al.*, 1971; *Derégnaucourt & Boillot*, 1982; *Malod & Boillot*, 1982; *Montadert et al.*, 1971]. The obliquity between the main rift directions, the trend of the oceanic spreading centre, and the direction of the later compression [e.g., *Boillot et al.*, 1971; *Derégnaucourt & Boillot*, 1982; *Jabaloy et al.*, 2002; *Jammes et al.*, 2009; *Rosenbaum et al.*, 2002; *Vergés & García-Senz*, 2001] permitted the preservation of the different stages of an almost complete orogenic cycle.

2.1) Mesozoic extension: the Bay of Biscay rift

The Iberian rift systems [*Salas et al., 2001*; *Salas & Casas*, 1993; *Tugend et al.*, 2015b; *Vergés & García-Senz.*, 2001] developed during Mesozoic transtension/extension linked to the formation and propagation of the Atlantic and Tethys oceans and the development of the European-Iberian plate boundary. It is widely agreed that

the Bay of Biscay formed as a branch of the southern North Atlantic rift system [*Malod & Mauffret, 1990; Roest & Srivastava*, 1991; *Ziegler*, 1988]. Offshore, the fingerprints of the Mesozoic extension are preserved within the structure of the North Iberian and the North Biscay conjugate margins [e.g., *Boillot et al.*, 1971; *Fernández-Viejo et al.*, 2011; *Montadert et al.*, 1971; Riaza, 1996; *Roca et al.*, 2011; *Thinon et al.*, 2003] (Figure 2a). Onshore, within the Pyrenean-Cantabrian realm, Mesozoic remnants extensively outcrop in the Pyrenees [e.g., *Jammes et al.*, 2009; *Lagabrielle et al.*, 2010; *Teixell*, 1998; *Vergés et al.*, 1995] and in the Basque-Cantabrian Zone, in the eastern Cantabrian Mountains [e.g., *Espina*, 1997; *Quintana*, 2012]. In contrast in the Asturian Massif, in the western Cantabrian Mountains, Mesozoic outcrops are very limited [*Virgili et al.*, 1971] (Figure 2a and b).

2.1.1) The post-Variscan wrench cycle and Permo-Triassic rift

During the Stephanian to early Permian, a tectono-magmatic wrench cycle, responsible for a major system of shear zones along the northern Iberian domain, developed during the post-orogenic collapse of the Variscan orogen [*Matte*, 1991; *Ziegler*, 1988; *Ziegler & Dèzes*, 2006]. In the Cantabrian Mountains, three main sequences, including continental deposits from the Gzhelian to the Lower Permian have been recognized [*Martínez-García*, 2004]. An early Permo-Triassic rift has been suggested based on the presence of Permo-Triassic sedimentary sequences onshore in northwestern Iberia [e.g., *Espina*, 1997 *Martínez-García*, 1983; *Pieren et al.*, 1995; *Suárez-Rodríguez*, 1988] (Figure 2b). NW-SE and NE-SW structures controlled the structure of grabens and the half-grabens developed during this period [*Espina*, 1997; *García-Mondéjar et al.*, 1986; *Lepvrier & Martínez-García*, 1990; *Suárez-Rodríguez*, 1988]. *Zamora et al.* [2017] defined the offshore Asturian Basin as a Permo-Triassic pre-rift salt basin developed during an early stage of crustal stretching.

Following the Permo-Triassic rift, a period of thermal subsidence affected the northern Iberian rifts during the Lower and the Middle Jurassic, leading to a general transgression and the development of characteristic marine facies that are progressively younger from west to east [*Quintana*, 2012; *González-Fernández et al.*, 2014; *Riaza*, 1996]. These sediments, including dolomites, limestones and calcareous claystones, have been interpreted as part of the pre-rift units imaged in the Basque-Cantabrian Basin and in the Asturian Basin [e.g., *Cadenas & Fernández-Viejo*, 2017; *Espina*, 1997].

2.1.2) The Late Jurassic to Early Cretaceous hyperextension processes

From the Late Jurassic to the Early Cretaceous, rifting processes in the southern North Atlantic rift system evolved progressively from south to north, leading to mantle exhumation and to the northward propagation and opening of the Southern North Atlantic ocean [e.g., *Dean et al.*, 2000; *Malod & Mauffret*, 1990; *Péron-Pinvidic et al.*, 2007; *Pitman & Talwani*, 1972; *Sibuet et al.*, 2007; *Srivastava et al.*, 2000; *Tucholke et al.*, 2007]. A major rifting event developed in the northern Iberian rift systems during this period [e.g., *Boillot et al.*, 1979; *Derégnaucourt & Boillot*, 1982; *García-Mondéjar*, 1996; *Montadert et al.*, 1971; *Tugend et al.*, 2014]. The strain partition that governed the polyphase extension led to the formation of strongly segmented rift systems, including disconnected hyperextended basins separated by N-S transfer zones [*Jammes et al.*, 2009; *Tugend et al.*, 2015b]. A first event of hyperextension occurred from the Barremian/Valanginian to the Aptian in the Bay of Biscay rift system, and was overprinted by a second event, which was better recorded in the Pyrenean-Basque-Cantabrian rift system, where these processes spanned from the Aptian to the Early Cenomanian[*Jammes et al.*, 2009; *Tugend*

et al., 2014]. In the Bay of Biscay rift, hyperextension processes included crustal thinning and mantle exhumation [*Tugend et al.*, 2014]. During this period, the Armorican Basin [*Montadert et al.*, 1971; *Thinon et al.*, 2002], the Asturian Basin [*Boillot et al.*, 1979; *Cadenas & Fernández-Viejo*, 2017; *Riaza*, 1996] and the Parentis Basin [*Bois et al.*, 1997; *Ferrer et al.*, 2008; *Jammes et al.*, 2010; *Pinet et al.*, 1987] developed as major rift basins (Figure 2a). *Tugend et al.* [2015a] interpreted the Parentis Basin as rift basin developed on top of a hyperthinned domain and defined a syn-hyperextension unit spanning from the Valanginian to the Aptian. In the Armorican Basin, *Thinon et al.* [2002, 2003] interpreted the emplacement of an allochthonous unit on top of exhumed basement during the Aptian. In the Asturian Basin, *Cadenas & Fernández-Viejo* [2017] interpreted a syn-rift unit spanning from the Late Jurassic to the Barremian.

In the Aptian, the reorganization of the African and European plates [*Rosenbaum et al.*, 2002] led to a complex stress field and the counterclockwise rotation of the Iberian plate [*Gong et al.*, 2008] and related movements between neighboring short-lived microplates [*Vissers & Meijer*, 2012]. This complex geodynamic evolution, together with the uncertainties about the origin and the age of M-series magnetic anomalies, has led to a long-lived controversy between plate kinematic and geological models concerning the rotation and the position of Iberia from the Late Jurassic to the Early Cretaceous [*Barnett-Moore et al.*, 2016].

2.1.3) Seafloor spreading within the Bay of Biscay and thermal subsidence in adjacent rift basins

The evolution of lithospheric breakup in the southern North Atlantic and the precise age of formation of the first oceanic crust in the Bay of Biscay are disputed. This is mainly because of the uncertain nature and age of the oldest linear magnetic anomalies attributed to the M-series along the Iberia-Newfoundland margin [e.g., *Bronner et al.*, 2011; *Nirrengarten et al.*, 2017; *Sibuet et al.*, 2007]. In the Bay of Biscay, such anomalies have been identified [*Roest & Srivastava*, 1991; *Sibuet et al.*, 2004] (displayed in green in Figure 2a), and further works showed that they fall onto thinned continental crust and exhumed mantle [*Thinon et al.*, 2003; *Tugend et al.*, 2014]. The Bay of Biscay V-shaped oceanic basin has been interpreted to develop during a short-lived Mid-Cretaceous (Latest Aptian to Albian) to Late Cretaceous (Campanian) seafloor spreading episode [*Sibuet & Collette*, 1991; *Sibuet et al.*, 2004]. The A34 magnetic anomalies are the only anomalies that are widely recognized and accepted as oceanic anomalies [*Srivastava et al.*, 1990] (displayed in blue in Figure 2a). Basaltic rocks interpreted as oceanic crust were drilled at Deep Sea Drilling Project Site 118 [*Laughton et al.*, 1972] (Figure 2a).

During this time span, a major period of thermal subsidence governed the evolution of the Asturian and the Parentis Basin in the North Iberian margin, where early stages of diapir emplacement occurred, and the Armorican Basin, in the northern Bay of Biscay margin [*Cadenas & Fernández-Viejo*, 2017; *Ferrer et al.*, 2008; *Thinon et al*, 2002; *Tugend et al.*, 2015a]. In the Asturian Basin and in the Armorican Basin, the breakup unconformity has been ascribed to the Aptian [*Cadenas & Fernández-Viejo*, 2017; *Thinon et al*, 2002].

2) The compressional reactivation of rift systems and the development of the Pyrenean-Cantabrian orogen

The prevailing extensional stress field was modified by the onset of the collision between the Iberian and the European plates in the Late Cretaceous. This collision lasted until the early Miocene [*Vergés et al.*, 2000]. At that time, the Iberian-European plate boundary became inactive and Iberia was incorporated into the European plate [*Roest & Srivastava*, 1991]. During the Alpine orogeny, the Bay of Biscay and the Pyrenean-Basque-Cantabrian rifts were reactivated to various extent, generating the present-day Pyrenean-Cantabrian orogen. North Iberia is classically interpreted to show from west to east a transition between incipient oceanic underthrusting/proto-subduction and complete continent-continent collision (the Pyrenees) [*Álvarez-Marrón et al.*, 1996; *Boillot et al.*, 1979; *Choukroune* and *ECORS Team*, 1989; *Fernández-Viejo et al.*, 1998; *Roca et al.*, 2011]. A crustal root developed beneath the collisional chain is well-known in the Pyrenees [*Choukroune* & *ECORS Team*, 1989; *Gallart et al.*, 1981], and extends westwards, although much smaller, within the Basque-Cantabrian Basin [*Pedreira et al.*, 2003, 2007] and beneath the summits of the Cantabrian Mountains [*Fernández-Viejo et al.*, 2000; *Pulgar et al.*, 1996; *Ruiz*, 2007].

During the Alpine compression, the North Biscay margin underwent minor tectonic reactivation [*Thinon et al.*, 2001]. In contrast, its conjugate to the south, the North Iberian margin, exhibited various stages of inversion due to the final docking of Iberia to Europe. Most of the compression offshore was accommodated through the formation of an accretionary wedge, now buried at the northern front of the continental slope [*Álvarez-Marrón et al.*, 1997; *Gallastegui et al.*, 2002; *Fernández-Viejo et al.*, 2012] and the southward underthrusting of a part of the distal domain beneath the platform [*Fernández-Viejo et al.*, 2012; *Roca et al.*, 2011]. The underthrusting led to crustal thickening and the uplift of the Cantabrian Mountains [*Alonso et al.*, 1996; *Fernández-Viejo et al*., 2000; *Pedreira et al.*, 2003; *Pulgar et al*., 1996] (Figure 2a). Meanwhile, the Asturian Basin and the Parentis Basin within the continental platform were slightly reactivated through the mild inversion of the main normal faults, the development of related folds, and the squeezing of diapiric structures [*Cadenas & Fernández-Viejo*, 2017*; Ferrer et al*., 2008; *Gallastegui et al.*, 2002]. Age-dated syn-orogenic units have been ascribed to the Middle Eocene to Lower Miocene within the accretionary wedge [*Álvarez-Marrón et al.*, 1997], to the Upper Cretaceous to Middle Miocene in the Parentis Basin [*Ferrer et al.*, 2008] and to the Upper Eocene to Lower Miocene in the Asturian Basin [*Cadenas & Fernández-Viejo*, 2017; *Gallastegui et al*., 2002].

Gallastegui et al. [2002] and *Pedreira et al.* [2015] estimated 96-98 km of shortening from the restoration of a complete section through the Cantabrian Mountains and the central part of the North Iberian margin. Further, east, within the Basque-Cantabrian Zone and the Parentis Basin, *Quintana et al.* [2015] calculated 122 km of shortening. In the Parentis Basin, the pre-Cretaceous restoration proposed by *Vergés & García-Senz* [2001] involves little inversion. In the eastern part of the collisional chain, in the Pyrenees, variable shortening values have been estimated ranging from 80 km to 147 km [e.g., *Mouthereau et al.*, 2014; Muñoz, 1992; *Teixell et al.*, 2016; *Vergés et al.*, 1995; *Teixell*, 1998].

2.3) The Asturian Basin as a major rift basin and the Mesozoic fossil remnants onshore in the western Cantabrian Mountains

The offshore Asturian Basin has been interpreted as a mildly inverted asymmetric rift basin filled by a sedimentary sequence including sediments from the Triassic to the Quaternary [*Cadenas & Fernández-Viejo*, 2017; *Boillot et al.*, 1979; *Gallastegui*, 2000; *Riaza*, 1996]. *Cadenas & Fernández-Viejo* [2017] interpreted a deep E-W basin bounded southwards by a major north-dipping normal fault and estimated its depth at the main depocentre as more than 10 km. In the southernmost continental platform of the central North Iberian margin, several exploration boreholes were drilled [*Cadenas & Fernández-Viejo*, 2017; *Gutiérrez-Claverol & Gallastegui*, 2002; *Lanaja*, 1987]. Sediments recovered by boreholes include Carboniferous sandstones and limestones, Triassic anhydritic red clays and sandstones belonging to the Keuper facies, with Muschelkalk limestones interbedded. The Lower Jurassic sediments includes Hettangian dolomites and limestones and Liassic limestones. The Upper Jurassic to Lower Cretaceous heterogeneous siliciclastic units represent the thickest deposits. The Upper Cretaceous corresponds to turbiditic deposits that are unconformably overlain by Tertiary continental deposits, including sediments with ages ranging from the Palaeocene to the Lower Miocene.

Onshore, the Asturian Basin is also known as Gijón-Villaviciosa Basin, and crops out near the coast, including sediments from the Permian to the Upper Cretaceous [e.g., *Uzkeda et al.*, 2016; *Valenzuela et al.*, 1986] (Figure 2b). Continental deposits with volcanic elements constitute the Permian [*Martínez-García*, 1981; *Suárez-Rodríguez*, 1988; *Wagner & Martínez-García*, 1982]. Muschelkalk carbonates from the Middle Triassic are very restricted or absent [*Robles & Pujalte*, 2004; *Tejerina & Vargas*, 1980]. Upper Triassic sediments include claystones and siltstones, with gypsum and evaporites, and dolomites and limestones in the upper part, corresponding to Keuper facies [*Pieren et al.*, 1995; *Suárez-Rodríguez*, 1988]. NW-SE and NE-SW syn-sedimentary faults controlled the Permo-Triassic sedimentation in this basin [*Martínez-García*, 1983; *Suárez-Rodríguez*, 1988].The most relevant structure within this family is the Ventaniella fault (Figure 2b). This fault has been interpreted onshore as a polyphase structure that could date from the initial post-Variscan reorganization of the Iberian massif [*Matte*, 1991; *Julivert et al.*, 1971]. Offshore, this structure, also referred to as Cantabrian fault, has been mapped traditionally to follow the trace of the Avilés canyon [*Boillot et al.*, 1973; *Derégnaucourt & Boillot*, 1982; *Martínez-Álvarez*, 1968]. Recently, *Fernández-Viejo et al.* [2014] interpreted this fault as a major structure that separates two distinctive crustal domains with different seismic activity. These authors proposed a new submarine location for this structure, running N60ºW. The Lower to Middle Jurassic sediments correspond to a well-known marine sequence, which includes dolomites and limestones, displaying a maximum thickness of about 600 m [*González-Fernández et al.*, 2014; *Valenzuela et al.*, 1986]. The Upper Jurassic sediments includes continental deposits linked to a second rift event, and shallow marine and fluvial deposits developed during the Kimmeridgian-Tithonian transgressive event [*González-Fernández et al.*, 2014]. From the Tithonian to earliest Barremian, *González-Fernández et al*. [2014] recognized a period of erosion/non-deposition and defined an Upper Barremian to Aptian transgression accompanied by the deposition of marine facies. The Aptian-Albian and the Upper Cretaceous deposits, corresponding mainly to siliciclastic sediments with some calcareous levels, are very

scarce and disconnected. Locally, these sediments overlie unconformably the Palaeozoic basement [*González-Fernández*, 2004]. NW- WNW-E-W faults have been recognized as the main faults conditioning the structure of the Jurassic and the Cretaceous materials [*Lepvrier & Martínez-García*, 1990; *Uzkeda et al.*, 2016]. The E-W trending Llanera Fault is interpreted as the main structure controlling the geometry of the onshore Asturian Basin [*Alameda & Ríos*, 1962] (Figure 2b). This structure was subsequently inverted during the Cenozoic resulting on the uplift of the Mesozoic sediments, which were thrust over the Cenozoic sediments of the Oviedo Basin [*Alonso et al.*, 1996].

3) Methodology and terminology

3.1) Rift domain definition

We followed the rift domain definition proposed by *Tugend et al.* [2015a]. These authors define five structural domain, which are referred to as proximal, necking, hyperthinned, exhumed mantle, and oceanic domains (Figure 1a and b).

The proximal **domain** is characterized by minor lithospheric thinning that results in the formation of classical graben and half-graben basins [*Tugend et al.*, 2015a; *Sutra et al.*, 2013] (Figure 1b). The **necking domain** has been defined as the area where 30 (±5) km continental crust is thinned to about 10 km [*Péron-Pinvidic* & *Manatschal*, 2009; *Mohn et al.*, 2012; *Sutra et al.*, 2013] (Figure 1b). The crustal thinning results in the creation of accommodation space, recorded by progressive thickening of the syn-rift sequences and deepening of depositional environments, the shallowing of the Moho, and the deepening of the top basement [Tugend *et al.*, 2015a]. The limit of this domain may correspond to the taper break [*Osmundsen* & *Redfield*, 2011] (Figure 1a) which usually coincides with the coupling point [*Péron-Pinvidic et al.*, 2013; *Nirrengarten et al.*, 2016]. The coupling point represents the place where the crustal deformation changes from a decoupled mode, in which faults sole out in ductile layers in the crust, to a coupled mode, in which faults penetrate across the thinned crust directly into the mantle [*Sutra et al.*, 2013], due to the embrittlement of the crust [*Pérez-Gussinyé et al.*, 2001] (Figure 1a and b). The **hyperthinned domain** is defined as the area where the continental crust is thinned from about 10 km to zero, leading to the development of a substantial amount of accommodation space [*Tugend et al.*, 2015a] (Figure 1a and b). With further extension, mantle rocks may also be in the **exhumed mantle domain** (Figure 1a). Anomalous seismic velocity structures have been interpreted to indirectly indicate the presence of serpentinized mantle at many magma-poor rifted margins [e.g., *Dean et al.*, 2000; *Minshull*, 2009]. Local magmatic additions, continental-derived extensional allochthons, serpentinized mantle rocks, locally reworked in syn-tectonic breccias, and sag-type basins filled by thick aggradational and progradational sequences that wedge out oceanwards, are also typical features of this domain [*Tugend et al.*, 2015a] (Figure 1a). Finally, the establishment of stable oceanic spreading and the presence of seafloor-spreading magnetic anomalies characterize the **oceanic domain**. The landward limit of this domain remains strongly debated owing to the gradational character recently attributed to breakup [*Péron-Pinvidic & Manatschal*, 2009] and the uncertainties in the interpretation of magnetic anomalies within ultra-distal rifted margins [*Nirrengarten et al.*, 2017; *Sibuet et al.*, 2007].

3.2) Mapping approach

We have characterized the rift domains in the central and western North Iberian margin following the approach developed by *Tugend et al.* [2014; 2015a]. The main assumption behind approach is that in magma-poor, thermally equilibrated rifted margins, the creation of accommodation space (given by the rift-related deposits) can be considered as a first-order proxy for crustal thickness (Figure 1b). Because the compressional reactivation that affected the North Iberian margin was superimposed on the rift structures, the application of this methodology is challenging, particularly where the former margin structures were reactivated and the crust has been thickened [*Fernández-Viejo et al.*, 2012; *Gallastegui et al.*, 2002]. To overcome this challenge, our interpretations relied on the following aspects: **1)** crustal structure, crustal thickness and type of extensional setting (high versus low betta setting, Figure 1); **2)** total accommodation space (between sea level and top basement) and specifically rift-related stratigraphic architecture; and **3)** nature of top basement (stratigraphic or tectonic) and present-day structural boundaries of the domain (extensional fault, inverted fault, thrust).

We use the CS01 dense set of commercial 2D multichannel reflection profiles of a high quality, obtained from the National Hydrocarbon Archive of Spain as time migrated stacks. We interpreted five E-W seismic profiles and thirty-eight N-S seismic lines, together with twenty-two boreholes (Figure 2). *Cadenas & Fernández-Viejo* [2017] provide the acquisition and the processing parameters as well as a description of the quality of the seismic records (supporting information, Tables S1 and S2). One of the longest N-S profiles that extends out for 107 km from the continental platform to the abyssal plain (CS01-132) (Figure 2) was post-stack depth migrated.

Seismic interpretation of the first-order interfaces allowed the definition of the crustal structure. We mapped five primary interfaces within the studied area to define the crustal scale architecture and the accommodation space (Figure 3 and 4): the seafloor, the base of the syn-orogenic deposits, the base of the post-hyperextension sediments, the top of the seismic basement, and seismic Moho. If the top of seismic basement corresponds to the base of sedimentary infill, these five interfaces enable us to define variations in crustal and sediment thickness of the rift-related deposits and the syn-orogenic deposits. In the central part of the North Iberian margin, the seismic Moho is not traceable, so we interpreted this interface from the integration with previous seismic velocity models from the ESCI-N and the MARCONI projects. We used IAM-12, ESCIN-3.1 and ESCIN-4 models from *Fernández-Viejo et al*. [1998], the ESCIN-3.3 model from *Ayarza et al.* [1998] and the MARCONI-1, MARCONI-6, MARCONI-4 and MARCONI-8 models from *Ruiz* [2007] (see inset in Figure 3). We have used these models to determine the two-way travel time of the Moho interface. The time conversion was gridded and the resulting data were extrapolated and superimposed on to the seismic sections (Figures 3 and 4).

Interpretation of the main seismo-stratigraphic sequences and the major structures allowed the definition of the stratigraphic architecture (Figure 5). These seismo-stratigraphic sequences are then related to the major tectonic events developed within the North Iberian margin as: **1)** the post-tectonic unit, developed during the passive margin stage; **2)** the syn-orogenic and the pre-orogenic units, related to the Alpine orogeny; **3)** the post-/syn-/ and pre-hyperextension units, linked with the main rifting event; and **4)** the seismic basement. A

detailed description of the seismic facies and the age of these units, as well as the seismic to well ties used to define the time constraints, is provided by *Cadenas & Fernández-Viejo* [2017]. A 3D analysis based on some boreholes allowed us to constrain the spatial variation of sediment thickness interpreted as part of the syn-orogenic and syn-hyperextension and post-hyperextension units (Figure 6 and 7). We represented the well records in terms of tectonic units after analysing the stratigraphic reports and defining the main seismo-stratigraphic units from the development of seismic to well ties and the correlation of the time constraints noted in the boreholes with the seismic facies observed within the seismic profiles.

Isopach maps developed from the first-order interfaces provided further constraints on local and regional changes in crustal and sedimentary thickness (Figure 8 and 9). To build these maps, we gridded the seafloor and the top of the seismic basement interpreted from the seismic data and the time converted seismic Moho from all the available velocity models. Using these surfaces and the CS01 migration velocities, we developed a velocity model and we depth converted the top of the seismic basement and the seafloor. From the combination of the resulting basement interface and the gridded refraction Moho, we developed a crustal thickness map (Figure 8). The subtraction of the depth converted top of the seismic basement and the seafloor defined the sediment thickness variations (Figure 9). Mapped crustal and sedimentary thicknesses also include the effects of inversion and crustal thickening during convergence. Thus, the present-day value of crustal thickness represents an upper limit, that locally reflect crustal thickening of previously extended crust due to reactivation.

Since the North Iberian margin is now, albeit submerged, part of the Pyrenean-Cantabrian orogen, our analysis of rift domains had to include the onshore Cantabrian Mountains, to understand better the influence of rift inheritance on the margin inversion. Onshore, rift domains are mapped based mainly on the analysis of the crustal thickness obtained from published wide-angle/refraction P-wave velocity models (Figure 10). We used the models developed for the westernmost area from *Córdoba et al.* [1987] and *Tellez* [1993], the IAM-12 and ESCIN-4 profiles, Profiles 1-5 from *Fernández-Viejo et al.* [1998, 2000], Profiles 1 and 6 from *Pedreira et al.* [2003], and the MARCONI-1 profile from *Ruiz* [2007] (see inset in Figure 10).

4) Structure and characterization of rift domains in the central and western North Iberian margin

The interpretation of the seismic profiles and the boreholes have revealed broad structural variability within the margin (Figures 3,4 and 5). From the interpretation of the first-order interfaces and the main structural and stratigraphic features, we have distinguished four distinct areas: **1)** a synclinal basin developed on top of thick crust, within the continental platform of the western North Iberian margin (Figures 3a and Figure 5a); **2)** the deep and wide Asturian Basin overlying a highly attenuated crust, in the continental platform of the central North Iberian margin (Figure 3b and c, Figure 4, and Figure 5b); **3)** the Le Danois High basement block, within the shelf-break and the continental slope in the central North Iberian margin (Figure 3b and c and Figure 4); and **4)** the accretionary wedge within the abyssal plain (Figures 4 and 5c).

4.1) Crustal structure: Seismic interpretation of first-order interfaces

The **seafloor reflection** varies from 200 ms TWT on the shelf to 5800 ms TWT in the abyssal plain. It is flat in the central continental platform but shows a low, deepening to 1.2 s TWT in the deepest part of the Asturian Basin (Figure 3b). On the continental slope and around the Santander, Torrelavega, Llanes, Lastres, Gijón, and Avilés major submarine canyons, the bathymetry is largely controlled due to the abundance of mass-wasting processes and canyon deposits [*Ercilla et al.*, 2008].

The **base of the syn-orogenic deposits** can be recognized in the central North Iberian continental platform, where it is well imaged by a regional erosional truncation which represents an onlap surface towards the limbs and the hinge of the anticlines (Figures 3b, 4, and 5b). This surface is irregular and draws the shape of the Alpine folds beneath the bathymetric low recognized in the Asturian Basin. It deepens to 2 s TWT toward the synclines (e.g., Figure 5b between 25 and 30 km of distance) and shallows to 1 s TWT towards the hinge of the anticlines (e.g. Figure 5b between 30 and 40 km of distance). In the southernmost part of the continental platform, this surface displays a fan-shape geometry, deepening to 2.5 s TWT in the so-called Peñas Trough (e.g., Figure 3b, between SP 0 and 100). Over the hinge of the anticline developed in the hanging wall, this surface shallows to 0.3 s TWT (e.g., Figure 3b, SP. 150 to 200). Within the abyssal plain, this surface can be followed between 7 and 8 s TWT in the frontal and central part of the accretionary wedge (Figure 4 and 5c). At the toe of the slope, this surface cannot be identified confidentially due to complex reflectivity patterns (Figure 4 between SP. 2100 and 2500). It constitutes a planar onlap surface in the frontal part of the accretionary wedge and a wavy baselap surface in the northernmost thrust sheet (Figure 4 between SP. 500 and 3100).

The **base of the post-hyperextension sediments**, our third interface in the continental platform, can be recognized between 2 and 4 s TWT within the depocentres of the Asturian Basin, where it is defined by an unconformity which passes laterally to a correlative conformity (Figure 3b between SP 300 and 450). In this area, this surface is folded and cut by the inverted faults (e.g., Figure 3b between SP.500 and 700). Within the southern part of the continental platform, the poor quality of the seismic record hampers its recognition in some seismic sections (Figure 3b southwards of SP 100). Therefore, we used data from boreholes to estimate its position at about 3 s TWT [*Cadenas & Fernández-Viejo*, 2017]. In the northern part of the continental platform and in the eastern part of the Asturian Basin, the distinctive reflection fabric of the parallel-layered post-hyperextension unit and the poorly reflective syn-hyperextension unit, together with the local toplap geometry of the syn-hyperextension sediments, have been used to map this interface (Figure 3b between SP 800 and 1300 and Figure 3c respectively). In the eastern part of the Asturian Basin, this surface is located between 3 and 4 s TWT and affected by the Alpine structures (e.g. Figures 3c between SP. 2100 and 800). In the northern part of the platform, this planar and south-directed surface progressively shallows to less than 1 s TWT over the Le Danois High. In

the western North Iberian platform, it could be assigned to a local planar unconformity overlying the pre-hyperextension deposits at about 0.3 s TWT (Figures 3a and 5a).

The **top of seismic basement** can be reasonably well constrained. In the central part of the margin, where the rift-related sequences and the syn-orogenic deposits filling the Asturian Basin can be differentiated [*Cadenas* & *Fernández-Viejo*, 2017], this horizon has been interpreted at the base of the pre-hyperextension unit (Figure 4 and 5b). This planar surface deepens to 6 s TWT of depth at the main depocentre of the Asturian Basin (e.g., Figure 3c around SP. 1200) shallowing to 3-4 s TWT in the southernmost continental platform and to less than 0.5 s TWT toward the Le Danois High (e.g., Figure 3b around SP. 100 and 1400 respectively).In the western sector of the study area, where boreholes are very scarce, we map a planar top basement at the base of the undifferentiated sedimentary infill. This surface is located at about 1 s TWT in the shelf break and shallows progressively toward the south, reaching less than 0.3 s TWT (Figure 3a). This surface draws locally a low at about 3 s (TWT) at the central part of the platform (Figure 3a). The top basement on the continental slope is shallow, as suggested by the recovering of basement samples previously described on the northern slope of Le Danois High [*Boillot et al.*, 1979; *Gallastegui et al.*, 2002]. The steepness, the abrupt change in water depths, and the abundance of mass-wasting deposits hamper interpretation due to the resulting chaotic seismic character. However, intra-basement reflections were distinguished (Figure 3 and 4). Beneath the abyssal plain, the top of the seismic basement has been interpreted in previous studies as corresponding to the base of Upper Cretaceous pre-orogenic deposits within the accretionary wedge [*Fernández-Viejo et al.*, 2011; *Roca et al.*, 2011]. In the new seismic dataset, we have identified a deeper folded and thrust top of the seismic basement in the central part of the North Iberian margin (Figure 4) where the accretionary wedge is better developed [*Fernández-Viejo et al.*, 2012]. This surface can be traced with confidence at about 9-10 s TWT in the frontal part of the thrust sheets (Figure 5c). In the western part of the North Iberian margin, the accretionary wedge is narrow and less developed [*Álvarez-Marrón et al.*, 1997; *Fernández-Viejo et al.*, 2012]. At these longitudes, the seismic fabric of the thin sedimentary record sometimes displays similar patterns to those observed within the underlying basement (Figure 3a), making it difficult to define the boundary between the two units.

Finally, the **Moho** is the deepest horizon used, and it is not always conspicuous in the reflection profiles. Its low amplitude in the central part of the margin [*Álvarez-Marrón et al.*, 1996; ; *Cadenas* & *Fernández-Viejo*, 2017; *Fernández-Viejo et al.*, 2011; *Pulgar et al.*, 1996] has been attributed to a reduced contrast in velocities between the lower crust and the upper mantle [*Fernández-Viejo et al.*, 1998; *Ruiz*, 2007], probably due to the serpentinization of uppermost mantle rocks now underthrust beneath the slope and the platform [*Fernández-Viejo et al.*, 2012; *Roca et al.*, 2011]. The grid developed from the integration of the published refraction models defines a planar surface located at about 9.5 s TWT in the western North Iberian platform, deepening to 11 s TWT in the northern part of the seismic profiles (Figure 3a). In the central North Iberian margin, Moho is at 9.5 s TWT in the continental platform. It shallows to 8-9 s TWT beneath Le Danois High and deepens again along the continental slope, reaching 12 s TWT at the northernmost part of the seismic profiles (Figure 3b and 5c).

4.2) Spatial variations of crustal and sediment thickness

Figures 8 and 9 show isopach maps of the residual crustal thickness (RCT) and sediment thickness respectively. The observed trends depict the existence of distinctive domains resulting from different modes of deformation within the two segments.

In the western segment of the North Iberian margin, RCT contours trend in a NW-SE direction. The continental platform area corresponds to a domain of thicker RCT, with values decreasing from 28 km to 25 km northeastwards. The < 1 km thick sedimentary cover interpreted to be present in this area, has a less well-defined trend. Sediment thickness locally reaches a maximum value of about 7 km at the depocentre of the rift basin (Figure 9). This basin overlies thinned RCT with values ranging from 21 km to 24 km. At the foot of the continental slope, RCT is reduced to 12 km. This area of extreme crustal thinning is wide and trends in a NW-SE direction. Within the abyssal plain, data are very sparse but the basement is less than 10 km thick and the sedimentary cover less than 2 km thick.

In the central segment of the North Iberian margin, contour are irregular and short. RCT and sediment isopachs run in a NW-SE direction in the southernmost continental platform, turning into an E-W direction in the Asturian Basin, in the Le Danois High area and in the abyssal plain. In the landward part of the continental platform, the RCT is more than 20 km and typical sediment thickness ranges from 6 to 8 km. RCT is reduced to less than 15 km beneath the Asturian Basin, where sediments thicken to more than 9 km. At the main depocentre, the basin sediments reach a maximum thickness of 13 km. This deep trough overlies a seismic basement less than 11 km thick. This domain of highly attenuated RCT and the overlying deep trough widen progressively southeastwards. The RCT is thicker in the Le Danois High, varying between 20 km and 14 km from west to east. Less than 1 km of sediments are found at the top of the high. RCT is strongly reduced from 20 km to 12 km along the continental slope. In contrast to the western segment of the margin, the RCT thins over a short distance and contours trend E-W direction in this central segment of the margin. Within the abyssal plain, RCT is reduced from 10 km to less than 4 km, with the smallest values at around 5º W (Figure 8), where sediment thickness reaches a maximum value of about 10 km (Figure 9).

The transition between the western and the central segments of the margin regarding the RCT and the sediment thicknesses, and the trends of their contours, occurs between 5º30´W and 6º W. This area strongly modified by the Avilés canyon, shows ill-defined isopach patterns within the continental platform. RCT varies between 15 km and 17 km and the sedimentary cover seems to thicken. However, sediment thickness is strongly modified by the presence of slope and mass-wasting deposits.

4.3) Basin architecture, tectono-stratigraphic evolution and thickness variations of rift-related deposits

The transition between each structural domain identified along the North Iberian margin reflects major structural and stratigraphic variations. In some areas, major structures can be recognized. The architecture of each domain reveals a tectonic evolution conditioned by strain partitioning in both extensional and compressional settings. Of particular interest is the polyphase evolution of rifting, as shown by the age and the spatial distribution of rift-related deposits. Thickness variations of syn-rift sequences reveal rift-related accommodation space creation, indirectly suggesting variations in the amount of crustal thinning across the margin segments. Different rift stages governed by particular deformation modes can therefore be recognized along the overall area. The occurrence of two rift events and the polyphase evolution of rifting, including progressive stages governed by different modes of deformation, complicates the tectono-stratigraphic analysis of the whole margin due to the presence of diachronous seismic sequences. Thus, we refer to *rift-related deposits* related to the hyperextension processes that governed the main rift event, having in mind that they may have different ages from west to east across the margin (Figure 5).

4.3.1) The rift basin on the western North Iberian margin

The westernmost part of the continental platform, west of approximately 6ºW, is characterized by the presence of rift basins. A wide unnamed basin, reaching a maximum thickness of about 3 s TWT, equivalent to about 7500 m, and a width of about 15 km, stands out (Figures 5a and 9). Two major high angle normal faults (labelled as FT1 and FT2 in Figures 5a), limit the basin. Although some of the faults show a minor inversion, the majority preserved their extension geometry (Figure 3a and 5a). The main known structure within this area corresponds to the Cantabrian or Ventaniella Fault. This fault is almost vertical and poorly imaged in seismic profiles offshore. Trend variations in the reflections can be used to map this structure (Figure 3a). The location of this structure coincides with the area where the top basement deepens abruptly (Figure 3).

The basin and the presence of high-angle normal faults is interpreted as related to crustal stretching processes that caused minor crustal thinning. This interpretation is coherent with the presence of an underlying thick continental crust (Figure 3a).

The sedimentary infill of this basin (Figures 3a and 5a) includes a fan-shaped syn-tectonic unit with onlap geometries that is overlain by a flat unit (Figure 5a). The two units are separated by an unconformity (Figure 5a). The only available borehole in this area, Galicia-B2, located southeast of the main depocentre of this basin (Figure 6) drilled a Palaeozoic basement, ascribed to the Silurian-Devonian, at a depth of 1,490 m, covered by 108 m of azoic red siltstones, shales and sandstones, attributed from facies correlation to the Triassic or an older age. The red beds are overlain by 1,056 m of an heterogeneous unit composed by an upper level of sandy mudstones and sandstones, with claystones and siltstones, and limestones, containing foraminifera, algaes and megafossils. Based on the presence of foraminiferal forms like *Pseudocyclamina sp.*, *Choffatella sp.*, *Trocholina sp.*, *Tritaxia sp*, and algaes like *Mithocodium*, these carbonates are dated as Lower Cretaceous, between the Aptian and the Neocomian, in the palaeontological report provided with the well record. This report dated the sandy limestones drilled at the sea bottom as Upper Cretaceous (Cenomanian), relying in the presence of foraminifera

like *Orbitoling Globotruncana*, *Globigerina and Cuncolina* ,which is also supported by the occurrence of *Classopollis*, *Cyathidites and Cicatricosisporites* among the spores, and dinoflagellates like *Hystrichosphaeridium*, *Systematophora* and *Oligosphaeridrium.* The possibility of a younger age cannot be completely excluded due to the rare occurrence of questionable *Operculodinium* and *Tectatodinium* in the palynological samples and *Globigerina* among the foraminifera.

From seismic to well ties, we interpret the main seismo-stratigraphic units, keeping in mind that these units would be much thicker in the main depocentre of the basin, where the sedimentary cover is about 7.5 km thick, than in the area where the well was drilled, recovering 1489 m of sediments. We included the Triassic deposits drilled in the well record into the fan-shaped unit identified within the seismic records that we interpret as a pre-hyperextension unit (Figure 5a). . We cannot exclude the possibility of other younger Mesozoic deposits within this sequence. The Lower Cretaceous sediments, including Aptian deposits, would be part of the flat unit that we interpret as a post-hyperextension unit.

4.3.2) The hyperthinned Asturian Basin on the central North Iberian margin

The continental platform in the central North Iberian margin, east of 5º30´W, is occupied by the major Asturian Basin (Figure 3b and c, Figure 4 and Figure 5b). The Asturian Basin is imaged as an E-W/ESE-WNW asymmetric rift basin with a maximum sedimentary thickness of about 6 s TWT at its main depocentre (Figure 3b and c and Figure 5b), equivalent to about 13.5 km (Figure 4). We interpret this geometry as controlled by two main normal faults that are now inverted (F1 and F2 in Figures 3b, 4 and 5b). The F1 extensional inverted fault appear as the main structure that controlled the morphology of the main depocentre (Figure 9) and the thickness of the syn-hyperextension unit (e.g., Figure 4). The F3, F4 and F5 faults could be related to the evolution of the northern part of the basin and the Le Danois High (Figure 3b and 4).The compressional overprint was limited to partial inversion and steepening of the extensional structures, the formation of a few minor reverse faults together with the development of related growth anticlines affecting the sedimentary cover, and the squeezing of diapirs (Figure 4). The sedimentary record has been divided into six seismic units according to the three main tectonic events developed in the margin [e.g., *Boillot et al.*, 1979; *Derégnaucourt & Boillot*, 1982] (Figure 5b). From top to bottom, we distinguish: **1)** the post-tectonic unit; **2)** the syn-orogenic unit; **3)** the pre-orogenic unit; **4)** the post-hyperextension unit; **5)** the syn-hyperextension unit; and **6)** the pre-hyperextension unit. Underlying these units, we distinguish the seismic basement. The Upper Eocene to Lower Miocene syn-orogenic deposits are much thinner than the rift-related deposits. Overlying the post-hyperextension and pre-orogenic units developed in the Asturian Basin from the Aptian to the Albian and from the Late Cretaceous to the Palaeocene, respectively, syn-orogenic sediments display onlap geometries toward the hinges and the limbs of the growth anticlines, thickening towards the synclines (e.g., Figure 4, between SP. 700 and 1400). The main syn-orogenic depocentre, filled by more than 3200 m of syn-orogenic sediments, corresponds to the so-called Peñas Trough. This trough, located in the southernmost part of the continental platform, developed in the footwall of the F1 inverted extensional fault [*Cadenas & Fernández-Viejo*, 2017; *Gallastegui et al.*, 2002] (Figure 4, between SP. 0 and 500).

In the southernmost part of the continental platform, the acoustic basement is interpreted to image a Palaeozoic basement overlain by Triassic sediments (Figure 5b). Borehole Mar Cantábrico-K1 reached a Carboniferous Palaeozoic basement at 3103 m, overlain by 600 m of Triassic carbonates and claystones with anhydrite (Figure 6). Therefore, we suggest that this area preserves the deposits related to the Permo-Triassic rift, and was subsequently overprinted by the major Late Jurassic to Early Cretaceous rift..

The Early to Middle Jurassic pre-hyperextension seismo-stratigraphic unit (Figure 5b) includes Liassic limestones, drilled in borehole Mar Cantábrico-K1 (Figure 6). The interpretation of a continuous pre-hyperextension unit overlying the seismic basement define a stratigraphic contact between the sedimentary cover and the underlying basement (Figure 5b). Nevertheless, in some profiles this unit cannot be recognized clearly so the nature of the top of seismic basement remains uncertain in some places (Figure 3c).

The syn-hyperextension unit is attributed to image the Late Jurassic to the Aptian sediments. It is interpreted in the seismic records as a thick wedge-shaped unit that reaches a maximum thickness of 4.1 s TWT (Figure 3b) equivalent to more than 11 km (Figure 4) at the main depocentre of the Asturian Basin. Boreholes Mar Cantábrico-K1 and Mar Cantábrico-M1 drilled 1790 m and 2837 m respectively, of siliciclastic sediments that we attribute to an heterogeneous syn-hyperextension unit (Figure 6). The thick syn-hyperextension sedimentary unit reflects a major event of creation of accommodation space in the Asturian Basin. Figure 7 displays a 3D view of thickness variations of the main seismic units along the trace of nine representative boreholes. The syn-hyperextension unit thickens toward the east and north (Figure 7). At the main depocentre of the Asturian Basin, this unit is 2256 m thick in borehole Mar Cantábrico- H1X and 2500 m thick in borehole Asturias-D2 (Figure 6 and 7). Within the continental platform, boreholes record progressive eastward thickening of the Upper Jurassic to Lower Cretaceous sediments identified as part as the syn-hyperextension unit. In the westernmost part, borehole Asturias E-1 drilled 1391 m, while at the easternmost part, borehole Mar Cantábrico-M1 recovered 2244 m.

We interpret the Aptian to Albian sediments as part of the post-hyperextension unit within the Asturian Basin (Figure 5b). Borehole Asturias-D2 drilled 900 m of Aptian to Albian deposits, borehole Mar Cantábrico H1X drilled 1200 m, while borehole Águila-1 recovered 2115 m (Figure 6 and 7). . The thickness of the Aptian-Albian sediments that we interpret as post-hyperextension deposits suggests major creation of accommodation space related to thermal subsidence of this basin.

The presence of such a thick basin on top of thinned continental crust, (Figure 3b and c and Figure 4) suggests an extreme crustal thinning. The thick Upper Jurassic to Lower Cretaceous syn-hyperextension unit recorded major tectonic subsidence, supporting this thinning. Thus, the Asturian Basin can be considered as a hyperthinned rift basin formed during a major rifting period spanning from the Late Jurassic to the Barremian. This event overprinted the Permo-Triassic rift event.

4.3.3) The Le Danois basement block on the central North Iberian margin

The Le Danois High represents a continental block that is thicker than the adjacent basement blocks to the north and to the south (Figures 3b c and 8).The top basement with this block is tilted eastwards (Figures 3c

and 4). In the seismic profiles located between 5ºW and 4º20´W, the top basement is interpreted at less than 1s TWT (Figure 3b). Eastwards of 4º20´W, the top of the seismic basement is interpreted at about 3 s TWT (Figure 3c). This basement high separates the Asturian Basin from the abyssal basin (Figure 4). This block hosts a small basin, bounded by the F3 and F4 faults (e.g., Figure 4). This basin widens towards the east (Figures 3 b, c, and 9). Flooring this basin, we interpret an unconformity surface that locally truncates the underlying basement reflections (e.g., Figure 3c around SP. 700, and Figure 4 between SP. 1600 and SP. 1800). The reflections at the bottom part of the sedimentary cover onlap over this basal truncation (e.g., Figure 3b around SP. 1300). The origin of this unconformity, whether it is exhumation and/or erosion, is difficult to discern because of the lack of borehole data and the difficulty in correlating the stratigraphy of this area with the main depocentre of the Asturian Basin. The small inner trough is interpreted to be separated from the Asturian Basin by the F2 inverted fault and its related anticline, developed over a faulted horst structure (Figure 4). Reactivation and/or inversion of minor high angle normal faults modified the original rift structure in the southern-most part of the block in its western side (Figure 3b and 4).

The sedimentary cover and, particularly, the syn-hyperextension unit thin dramatically toward the Le Danois High (Figure 9). Based on the correlation of the seismic facies with those identified within the Asturian Basin, we interpret the base of the post-hyperextension and the base of the syn-orogenic unit, which define a thin and partially eroded post-hyperextension unit (Figure 3b and 4). This unit underlies an irregular syn-orogenic unit and unconformably overlies a thin syn-hyperextension unit. The thickness of both units increases towards the east (Figure 3b and c). The northern slope of the Le Danois High corresponds to the continental slope, and the wavy shape of the reflections suggest the presence of sediments dominated by mass-wasting processes. (e.g., Figure 3b between SP 1500 and SP 1800; Figure 3c, between SPs 300 and 100). We interpret some of the mass-wasting deposits to be interbedded within syn-tectonic sequences Therefore, mass-wasting processes could be interpreted as related to tectonic activity. At the toe of the slope, we recognized mass-wasting deposits overlain by recent flat post-tectonic strata and interbedded within the syn-orogenic depostis, suggesting that the Alpine compression and uplift triggered the mobilisation of these sediments (e.g., Figure 5c).

4.3.4) The accretionary wedge in the Bay of Biscay abyssal plain

The accretionary wedge is deeply buried within the abyssal plain beneath the post-tectonic flat-layered unit (Figure 5c). This structure thickens and widens to the east, where more widely spaced north-verging thrust structures are observed [*Fernández-Viejo et al.*, 2012]. Underlying a fan-shaped syn-orogenic unit, we interpret a well-defined pre-orogenic/post-hyperextension unit, which unconformably overlies an undifferentiated Mesozoic unit (Figure 5c). The strong segmentation of the margin structure and the lack of direct data preclude lateral correlations and the definition of precise time constraints for these units. *Álvarez-Marrón et al.* [1997] and *Fernández-Viejo* [2011] interpreted a pre-orogenic unit, which they attributed to the Upper Cretaceous to Palaeocene-Eocene, and a syn-orogenic unit, which they ascribed to the Middle Miocene to Lower Miocene. We tentatively ascribed the undifferentiated Mesozoic unit that we identified underlying the pre-orogenic/post-

hyperextension unit to the Early Cretaceous and we relate this unit is related to the hyperextension processes. The basement has been interpreted to transitional crust in the central part of the margin and oceanic crust in the western part [*Álvarez-Marrón et al.*, 1996; *Fernández-Viejo et al.*, 1998]. In the central North Iberian margin, the presence of an extremely thinned crustal domain and the proposed existence of an exhumed mantle domain [*Roca et al.*, 2011; *Tugend et al.*, 2014] call for high degrees of crustal thinning and possibly even mantle exhumation.

- The northermost fault within the accretionary wedge corresponds to the Biscay Wedge Front [*Fernández-Viejo et al.*, 2012]. This south dipping thrust trends in an E-W direction and limits the accretionary wedge, marking the northern deformation front of the Pyrenean-Cantabrian range offshore. The southward limit of the accretionary wedge at the backstop is not well-constrained. Within this area, the southernmost thrust, which is recognized in reflection profiles by a change in the trend of reflectivity patterns (Figure 4) has been mapped at the toe of the slope (Figure 8).(Figure 11).

5) Crustal thickness compilation over the Cantabrian Mountains

Figure 10 shows the depth of the crust-mantle boundary onshore and the extension of the crustal root beneath the Cantabrian Mountains. The figure shows a western domain where crustal thickness varies between 27 and 30 km, and an eastern domain, where the crust is more than 40 km thick, corresponding to the crustal root. The crustal root extends between 4ºW and 6ºW. It trends in a NW-SE/E-W direction in between and in a N-S direction at the edges. Despite the low density of wide-angle seismic data on this area, we can tentatively suggest that major variations in the shape and the extent of the crustal root and thus, the transition between the western and the eastern crustal domains, occurs in the vicinity of the trace of the Ventaniella Fault (Figure 10).

6) Rift domains in the central and western North Iberian margin and in the western Cantabrian Mountains: a new map

Following the analysis and the study of all the geological and geophysical data and the observations outlined before, we propose a new rift domain map within the central and western North Iberian margin and within the western Cantabrian Mountains (Figure 11).

The **proximal domain** includes most of the westernmost part of the continental shelf (Figure 11). A shallow rift basin bound by high-angle syn-sedimentary faults developed on this area. Its outer limit, defined as the location where the top of seismic basement deepens abruptly, runs parallel to the Cantabrian Fault offshore that constitutes now the distal structural boundary of this domain. Onshore, this domain includes the western crustal domain identified beneath the Cantabrian Mountains, where crustal thickness varies between 27 and 30 km.

The **necking domain** is irregular (Figure 11). In the western North Iberian margin, it is narrow and trends in an NW-SE direction. Its distal limit is marked by the area in which the top basement deepens from 5 to 6 s TWT, marking a crustal thickness reduction of about 10 km (displayed in light purple in Figure 11) and the southernmost thrust interpreted within the accretionary wedge. In the central part of the margin, the F1 inverted fault constitutes the seaward limit of the NW-SE trending necking domain (Figure 11). In this area, the NW-SE

necking domain widens to 38-63 km, ending abruptly towards the hyperthinned domain. Onshore, we propose that the necking domain includes the eastern thicker domain identified beneath the Cantabrian Mountains, where the crust is more than 40 km thick.

The V-shaped **hyperthinned domain**. beneath the Asturian Basin is bound by the inverted normal faults F1 to the south and F2 to the north (Figures 11). To the west, this domain ends abruptly at around 5º30´W of longitude, where we suggest the presence of a N-S transfer zone (Peñas Transfer Zone in *Cadenas*, 2017). To the east, the basin is limited by the Santander transfer zone [*Roca et al.*, 2011] (Figure 11).

Within the abyssal plain, we map a former **hyperextended domain** that includes the hyperthinned and the exhumed mantle domains undifferentiated and possibly evolves to a truly oceanic basement towards the west (Figure 11). Part of these distal domains are interpreted to be now underthrust southward beneath the former basement due to the reactivation of the margin [; *Fernández-Viejo et al.*, 2012; *Roca et al.*, 2011; *Tugend et al.*, 2014]. The nature of the underthrust rift domains and their southern limit cannot be elucidated accurately. We have mapped a maximum area of underthrust rift domains (Figure 11) that accounts for the extent of the anomalous mantle velocities recognized in refraction studies [*Fernández-Viejo et al.*, 1998; *Ruiz*, 2007], that are attributed to serpentinization processes [*Fernández-Viejo et al.*, 2012].

Finally, the **oceanic domain** corresponds to the area with unequivocal A34 magnetic anomalies [*Sibuet* & *Collette*, 1991; *Sibuet et al.*, 2004] (Figures 2a and 11) and where basaltic rocks were recovered at the westernmost corner of the Bay of Biscay (Figure 2a).

7) Discussion and geodynamic implications

7.1) Implications of this new mapping for the structure of the Bay of Biscay rift

7.1.1) The rift basin within the proximal domain in the western North Iberian margin

The seismic data show a wide basin within the continental platform of the western segment of the North Iberian margin. Although minor Mesozoic basins have been previously recognized in the southernmost part of the continental platform [*Ayarza et al.*, 1998; *Boillot et al.*, 1973; *Martínez-Catalán et al.*, 1995], the presence of such a deep trough reaching 3 s TWT, or about 7.5 km at its main depocentre, has not been described in previous studies. The origin and the evolution of this basin remains unclear mainly because of the lack of direct data within the main depocentre that allow dating of the seismic units. We interpret that the development of this basin dates back to the Permo-Triassic rifting period based on the nearest borehole. The identification of a thick post-hyperextension unit reveals a long period of thermal subsidence during the evolution of this trough that we interpret to have occurred at least from Aptian onwards.

7.1.2) The Asturian Basin: a new hyperthinned domain within the rift system

We identified the Asturian Basin as being underlain by a hyperthinned continental crust (Figures 3, 4 and 8). Even if the crust has been locally thickened during convergence at deep crustal levels, no more than 12 km thick crust is observed now beneath the main depocentre (Figure 4 and 8). Structures that can account for the

extreme crustal thinning have not been deduced yet within the Asturian Basin. We propose that the main fault controlling crustal and sediment thickness variations within the Asturian Basin is the F1 normal inverted fault. As suggested by *Jammes et al.* [2010] in the Parentis Basin, the main thinning structure in the Asturian Basin is expected not to have seismic expression and could be, instead, related in depth with the major F1 normal fault.

Further studies are needed to constrain more accurately the limits of the Asturian Basin hyperextended domain, especially towards the east, where the Santander Transfer Zone [*Roca et al.*, 2011] links the Asturian Basin, the Parentis Basin and the hyperextended abyssal plain areas offshore with the Basque-Cantabrian Basin onshore (Figure 12).

7.1.3) The Le Danois High: a continental block or a thickened hyperextended domain?

The Le Danois High appears as a relatively thick basement block surrounded by hyperthinned domains on its southern and northern sides (Figure 8). This acoustic basement block appears as a necked area less thinned than the bounding hyperextended domains. The crustal block is limited southwards by the F2 normal fault. The southernmost thrust interpreted within the accretionary wedge, and the area where the basement deepens, due to a crustal thickness reduction of about 10 km (displayed in light purple in Figure 11), delineate its distal limit.

Samples of granulites reworked within Aptian and Albian breccias were recovered on the northern slope of Le Danois High [*Capdevila et al.*, 1980; *Fügenschuh et al.*, 2003; *Malod et al.*, 1982]. Fügenschuh *et al.* [2003] reported cooling ages for three samples (Figure 8) using fission tracks on apatites. The two samples dredged at the top of Le Danois High have cooling ages of 138 and 120 Ma respectively while the easternmost sample yields an age of 52 Ma. These authors proposed that the first two samples were exhumed during the main rifting phases, supporting the exhumation of lower crustal rocks during hyperextension, while the third was subsequently reheated due to the Cenozoic underthrusting. The presence of lower crustal rocks at the top of a basement high is an outstanding feature, which is still under debate. Two interpretations can be proposed to explain the structure of the Le Danois High:

1) the Le Danois High might be underlain by north-verging thrusts [*Boillot et al.*, 1979; *Gallastegui et al.*, 2002; *Malod et al.*, 1982; *Pedreira et al.*, 2015]; or **2)** it might correspond to a basement block of less thinned continental crust [*Cadenas* & *Fernández-Viejo*, 2017]. In the first interpretation, Le Danois High was a highly extended part of the margin prior to the reactivation. During the subsequent compressional reactivation, the stacking of hyperextended crust would have led to the crustal thickening. This hypothesis would explain the presence and the age of the granulites dredged at its northern slope. In this alternative second interpretation, the Le Danois High would represent a remnant of a basement high inherited from the rifting processes.

We favour to interpret the Le Danois High as a continental block inherited from the rifting stage based on the results of this study. The sedimentary infill of the small trough at the northern side of the Asturian Basin displays onlap geometries (Figure 3b between SP 1200 and SP 1400). A thin syn-hyperextension unit has been interpreted based on the wedge-shaped geometries identified within the depth migrated profile (Figure 4, between

SP 1500 and 1600). This geometry reveals the presence of an uplifted block to the north during hyperextension. Even if this infill was a passive post-hyperextension unit, Le Danois would be a continental block of less extended crust just prior to the compression. The presence of the Le Danois crustal block as an extensional relict, similar to a continental ribbon [*Lister*, 1986; *Péron-Pinvidic & Manatschal*, 2010], can explain the strong segmentation and the strain partitioning during both the extensional and the compressional events. Some structures (Figures 3b and c and 4) suggest that the block may have undergone rotation during the compression phase and its original trend might have been more oblique to the E-W trend of the margin.

7.1.4) The hyperextended domain within the Biscay abyssal plain

Within the abyssal plain, the distinction between the hyperthinned domain and/or the exhumed mantle domain is difficult. The nature of the basement within this area remains debated [*Roca et al.*, 2011; *Pedreira et al.*, 2015]. Velocities attributed to serpentinization related to mantle exhumation (Vp<8 km/s in Figures 3b and c, 4 and 11) [*Fernández-Viejo et al.*, 2012] have been identified beneath the continental platform and slope of the North Iberian margin [*Fernández-Viejo et al.*, 1998; *Ruiz*, 2007]. Based on gravity inversion results, *Tugend et al.* [2014] have interpreted that part of the basement of the abyssal plain might represent a former exhumed mantle domain. This former exhumed mantle domain is likely better preserved at the northern Biscay margin [*Thinon et al.*, 2003; *Tugend et al.*, 2014] and occurs as fossil remnants within the Pyrenean Basque-Cantabrian rift system [*Tugend et al.*, 2014]. However, the extent of the exhumed mantle domain has not been constrained accurately in the North Iberian margin. To add complexity, within the distal domains, there is an E-W variation on the nature of the basement. In the central part of the margin, the basement includes hyperextended domains [*Roca et al.*, 2011; *Tugend et al.*, 2014]. In the west, however, an oceanic basement has been recognized on previous studies [*Álvarez-Marrón et al.*, 1997; *Fernández-Viejo et al.*, 1998]. Due to this uncertainty, we mapped an undifferentiated hyperextended domain including extremely thinned continental crust and, possibly, areas of exhumed mantle.

7.2) Segmentation and partitioning of deformation within the central and western North Iberian margin

From this study, we can suggest that the Bay of Biscay rift was a complex and polyphase system. A remnants rift basin related to a Permo-Triassic rift are suggested in the western North Iberian margin. This rift event did not evolve into hyperextension. During the Late Jurassic to Early Cretaceous rift, hyperextension, exhumation, and the development of the major rift basins occurred within the central and eastern parts of the Bay of Biscay rift system (Figure 12). It was during this phase that the Asturian Basin developed fully in the central part of the North Iberian margin. Therefore, crustal thinning and related syn-hyperextension Upper Jurassic to Lower Cretaceous sediments overprinted the Permo-Triassic rift on this area . . In the Armorican Basin, an Aptian syn-hyperextension unit has been recognized [*Thinon et al.*, 2002; *Tugend et al*., 2015a]. A similar age could be proposed for the undifferentiated Mesozoic seismo-stratigraphic unit identified within the Biscay abyssal plain that overlies an extremely thinned continental crust (Figure 5c).

Thus, the central and western North Iberian margin preserves structures related to two polyphase rift events. All the structural and the stratigraphic variations observed within the margin suggest the presence of a N-S transfer zone which has not been described up to now, referred to as Peñas Transfer Zone in *Cadenas* [2017], but which may be located between 6ºW and 5º30´W (Figure 11). The presence of N-S to NNE-SSW trending structures, such as the Santander or the Pamplona and Toulouse transfer zones (Figure 12), have been already interpreted as a sign of rift segmentation within the Pyrenean-Cantabrian domain explaining the occurrence of disconnected hyperextended basins [*Larrasoaña et al.,* 2003;*Tugend et al.,* 2014]. We suggest that the transition from the hyperextended domain to the oceanic domain in the distal areas might occur within this transfer zone.

7.3) The role of rift inheritance on the compressional reactivation of the margin.

7.3.1) The hyperextended domains within the abyssal plain: the focus of the compressional reactivation

We suggest that the hyperextended domains focused subsequent compressional deformation [*Tugend et al*., 2014]. *Lundin* & *Doré* [2011] and *Péron-Pinvidic et al.* [2008] speculated that minor reactivation along the North Atlantic margins typically localized in the exhumed mantle domain. In the North Iberian margin offshore, especially within the central part of the margin, most of the compression was accommodated in distal domains by underthrusting of part of the hyperextended domains beneath the margin and by the development of an accretionary wedge. The accretionary wedge is wider and thicker in the central part of the margin; thrusts become more widely spaced and accompanied by the development of out of sequence structures [*Fernández-Viejo et al.*, 2012] (Figure 12). To the west, the wedge is narrow and thrust spacing is shorter [*Álvarez-Marrón et al.,* 1997; *Fernández-Viejo et al.,* 2012]. Some changes of the dimensions of the accretionary wedge occurs within the proposed transfer zone between 5´30 and 6ºW of longitude. This variation could also reflect the different nature of the underlying basement.

7.3.2) The buffering effect of the proximal domain: constraints imposed by the rifted crust into the development of a crustal root

The crustal variations between the proximal and the necking domains seems to influence greatly compressional reactivation. Offshore, this boundary runs parallel to the Cantabrian-Ventaniella Fault (Figure 11). Onshore, the Ventaniella Fault seems to limit the crustal root towards the west (Figure 10). We speculate that the disappearance of the root westwards of the Ventaniella Fault is directly related to the boundary with the proximal domain, and hence, a more rigid crustal block where underthrusting of the previously rifted margin was no longer possible. Therefore, we can suggest that the inherited rift architecture and in particular the necking domain might have controlled the geometry of the crustal thickening beneath the Cantabrian Mountains.

The Ventaniella Fault includes segments with different kinematics that were active at different stages during the evolution of the Iberian domain since the Permian. Thus, the segmentation and the strain localization complicate the study of the polyphase evolution of this fault, interpreted as a post-Variscan structure with a subsequent enigmatic activity during the Mesozoic extension and the Alpine compression [*Boillot et al*., 1971; *Julivert et al.*,

1971; *Lepvrier & Martínez-García*, 1990]. Offshore, the Ventaniella Fault trends in a NW-SE direction and separates a western seismically active crustal segment, from an eastern segment with less activity [*Fernández-Viejo et al.*, 2014]. Onshore, this fault shows a NW-SE trend and has a seismically active segment in its southern limit. Based on the structure and the architecture of the western North Iberian margin, the offshore trace of this fault now coincides with the limit between the proximal and the necking domains interpreted in this study. Onshore, we suggest that this fault delineates now the proximal-necking boundary, which acted as a rheological limit during the first compressional events, conditioning the development of the crustal root beneath the Cantabrian Mountains. With this interpretation, we propose that the Ventaniella Fault would be an Alpine reactivation of a NW-SE trending rift structure active since the Permo-Triassic rift. Reactivation would have been favoured by the obliquity between the fault trend and the N-S directed compression. Onshore, this fault shows a dextral strike-slip movement [*Marcos*, 1979], consistent with a N-S convergence [*Pulgar et al.*, 1999]. Further studies are required to: **1)** elucidate the origin, the evolution and the activity of this structure during the rift events; **2)** constrain the validity of its interpretation offshore as a continuation of the onshore Ventaniella fault, corresponding to a single structure or, perhaps more accurately, as a NW-SE fault system including different branches that where active at different times.

7.3.3) The buffering effect of the Le Danois High: the mild inversion of the Asturian Basin

The mild inversion observed in the sedimentary cover of the Asturian Basin is related to the presence of Le Danois crustal block bounding the basin to the north. This residual block of less thinned continental crust preserved the inner basin from the compressional deformation. The underthrusting of the hyperextended crust beneath the High and the development of an accretionary wedge at the toe of the slope accommodated most of the compressional deformation, resulting in a passive uplifting and a slightly reactivation of the whole area. In contrast to the Landes High, which acted as a regional buffer of compressional deformation [*Ferrer et al.*, 2008], Le Danois high acted as a local buttress hampering further inversion of the Asturian Basin. The link between these highs and their role during the extension and the subsequent compressional reactivation need to be further assessed.

8) Conclusions

In this study, we define rift domains along the central and western North Iberian margin. The transition between the different structural areas identified along the whole margin reflects major structural and stratigraphic variations. The distribution and the extent of these structural elements helps to define the main rift domains boundaries. We propose a new map showing the limits between proximal, necking, hyperthinned, hyperextended and oceanic areas within the central and western North Iberian margin. One of the main findings of this work is the definition of a hyperthinned domain in the continental platform of the central North Iberian margin and the characterization of the Le Danois High as a less thinned crustal block inherited from the rift development.

We show that the mapping of rift domains is a useful tool to predict the initial locus of inversion within rift systems. Such inversion has been studied previously in areas where reactivation was minor [*Kimbell et al.*, 2016; *Thinon et al.*, 2001; *Péron-Pinvidic et al.*, 2008].The distinctive compressional overprint observed along the

North Iberian margin makes this margin a remarkable setting to study the influence of rift structural inheritance on the subsequent compression. Although it has been proposed before that some of the lateral changes observed along the Pyrenean-Cantabrian orogen could be related to the initial rift structure [*Fernández-Viejo et al.*, 2012; *Roca et al.*, 2011] our work adds more insights into the role of rift inheritance on reactivation processes [*Mohn et al.*, 2014; *Tugend et al*., 2014]. We propose that indeed the former hyperextended and necking domain boundaries controlled the location of reactivation along the whole margin, playing an important role in the development of the current crustal architecture of the margin and of the Cantabrian Mountains. We draw the following conclusions:

1) The segmentation observed within the North Iberian margin results from a strong partitioning of deformation and a progressive strain localization during rifting that conditioned the subsequent compressional reactivation.

2) The hyperextended domain focused most of the compressional reactivation, which was mainly accommodated at a crustal scale through the formation of an accretionary wedge and the underthrusting of the hyperextended crust.

3) The necking area, and particularly the transition between the proximal and the necking domains, delineated now by the Cantabrian or Ventaniella fault, buffered the compressional reactivation. A distinctive crustal thickness gradient can be observed at both sides of this structure beneath the Cantabrian Mountains.

4) The presence of the semi-detached Le Danois continental block, analogous to a continental ribbon, in between two hyperextended domains hampers compressional reactivation of the related Asturian Basin, acting as local buttress.

The new rift domain map adds helpful clues to constrain restorations of the inverted margin, which can clarify the evolution of the Bay of Biscay-Pyrenean rift system during the compressional reactivation. Moreover, the mapping of rift domains is a powerful tool to unravel some of the features observed not only on the margin but also along the onshore Cantabrian Mountains, where Mesozoic remnants are scarce. Thus, it is important to consider that any further study in the central part of the inverted rift system must involve onshore and offshore areas, as both are now part of the same compressional belt.

The study in a more global sense shows the importance of rift inheritance during the earlier stages of compression or a margin reactivation, episodes that are normally erased through the evolution of an orogeny, but that mark the future development and the structure of the collisional chain.

Acknowledgements

No conflict of interest declared

This work has been financed by the Ministry of Science and Innovation of Spain through the Projects MARCAS: CTM2009-11522 and MISTERIOS: MINECO13-CGL2013-48601-C2-2-R and the Government of Asturias and the FEDER funds through the Project GEOCANTABRICA: GRUPIN14-044. P. Cadenas held a Severo Ochoa PhD grant from the Education Council of Asturias. This grant funded two short term stays of P. Cadenas in the National Oceanography Centre of Southampton and in the University of Strasbourg/EOST of Strasbourg. J. Tugend and G.

Manatschal are supported by the MM4 consortium. T. A. Minshull is supported by a Wolfson Research Merit award.
The CS01 2-D seismic data and the boreholes used in this study were purchased through the ATH (http://geoportal.minetur.gob.es/ATHvz/).The interpretation of the 2-D time migrated stacks and the boreholes was carried out using Kingdom and Petrel E&P softwares, which were provided by IHS and Schlumberger, respectively, as part of educational programmes. Maps were produced with ArcGIS-ESRI software.
The authors acknowledge the thoughtful and useful reviews provided by Webster Mohriak and two anonymous reviewers that helped to improve the early version of this manuscript. We thank the Editor Claudio Faccenna for handling the manuscript.

References

- Alameda, A., and J.M. Ríos (1962), Investigación del Hullero bajo los terrenos Mesozoicos de la costa Cantábrica (zona de Oviedo-Gijón-Villaviciosa-Infiesto), Empresa Nacional Adaro de Investigaciones Mineras, Madrid, 159 pp.
- Alonso, J.L., J.A. Pulgar, J.C. García-Ramos, and P. Barba (1996), Tertiary basins and alpine tectonics in the Cantabrian Mountains, NW Spain. In: Tertiary basins of Spain: the stratigraphic record of crustal kinematics, Edited by P. F. Friend and C. J. Dabrio, Cambridge University Press, Cambridge, 214-227.
- Álvarez-Marrón, J., A. Pérez-Estaún, J.J. Dañobeitia, J.A. Pulgar, J.R. Martínez-Catalán, A. Marcos, F. Bastida, P.A. Arribas, J. Aller, J. Gallart, E. Banda, M.C. Comas, and D. Córdoba (1996), Seismic Structure of the northern continental margin of Spain from ESCIN Deep seismic profiles, Tectonophysics, 264, 153-174.
- Álvarez-Marrón, J., E. Rubio, and M. Torne (1997), Subduction-related structures in the North Iberian margin, J. Geophys. Res., 102 (B10), 22,497-22,511.
- Ayarza, P., J. R. Martínez-Catalán, J. Gallart, J. A. Pulgar, and J. J. Dañobeitia (1998), Estudio Sísmico de la Corteza Ibérica Norte 3.3: A seismic image of the Variscan crust in the hinterland of the NW Iberian Massif, Tectonics, 17, 171-186.
- Barnett-Moore, N., M. Hosseinpour, and S. Maus (2016), Assessing discrepancies between previous plate kinematic models of Mesozoic Iberia and their constraints, Tectonics, 35, doi: 10.1002/2015TC004019.
- Boillot, G., P.A. Dupeuble, M. Lamboy, L. D´Ozouville, and J.C. Sibuet (1971), Structure et histoire géologique de la marge continentale au Nord de l´Espagne (entre 4º et 9º W), in: Historie structurale du Golfe de Gascogne, edited by: J. Debysier, X. Le Pichon and M. Montadert, Technip, París, V. 6-V6.52.
- Boillot, G., P.A. Dupeuble, M. Lamboy, I. Hennequin-Marchand, I., an J.P. Lepretre (1973), Carte géologique du plateau continental nord-espagnol entre le canyon de Capbreton et le canyon d´Aviles. Soc. Géol.France, 7, 15, 3-4: 361-391.
- Boillot, G., P. A. Dupeuble, and J. Malod (1979), Subduction and Tectonics on the continental margin off northern Spain, Marine Geology, 32, 53-70.
- Boillot, G., and N. Froitzheim (2001) Non-volcanic rifted margins, continental break-up and the onset of sea-floor spreading: some outstanding questions. In: Non-Volcanic Rifting of Continental Margins: A Comparison of Evidence from Land and Sea, Edited by R.C.L. Wilson, R.B. Whitmarsh, B. Taylor, & N. Froitzheim, Geol. Soc. London Spec. Pub., 187, 9-30, London, The Geological Society.
- Bois, C., O. Gariel, J.P. Lefort, J. Rolet, M.F. Brunet, P. Masse, and J.L. Olivet (1997), Geologic contribution of the Bay of Biscay deep seismic survey: summary of the main scientific results, a discussion of the open questions and suggestions for further investigation, Mém. Soc. Géol. France, 171,193-209.
- Bronner, A., D. Sauter, G. Manatschal, G. Péron-Pinvidic, and M. Munschy (2011), Magmatic breakup as an explanation for magnetic anomalies at magma-poor rifted margins, Nat. Geosci., 4, 549-553, doi: 10.1038/ngeo1201.
- Brune, S., C. Heine, M. Pérez-Gussinyé, S. V. Sobolev (2014), Rift migration explains continental margin asymmetry and crustal hyper-extension, Nature Communications, 5, doi: 10.1038/ncomms5014.

- Cadenas, P., and G. Fernández-Viejo (2017), The Asturian Basin within the North Iberian margin (Bay of Biscay): seismic characterization of its geometry and its Mesozoic and Cenozoic cover, Basin Research, 1-21, doi: 10.1111/bre.12187.
- Cadenas, P. (2017), 3D modelling of the Cantabrian margin between 3ºW and 8ºW. Geodynamic implications, PhD Thesis, pp. 212, University of Oviedo.
- Cadenas, P. & G. Fernández-Viejo (2018), A Geodynamic Approach, In: Geology of Iberia. A Geodynamic Approach, Edited by: Quesda, C. & T. Oliveira, Springer, Heildelberg.
- Capdevila, R., G. Boillot, C. Lepvrier, J. A. Malod, and G. Mascle (1980), Metamorphic and plutonic rocks from the Le Danois Bank (North Iberian Margin). In: Comptes Rendus Hebdomadaires des Seances de L´Academie Des Sciences, Serie D, 291,317-320.
- Choukroune, R., and ECORS Team (1989), The ECORS- Pyrenean deep seismic profile reflection data and the overall structure of an orogenic belt, Tectonics, 8, 23-39, doi: 10.1029/TC008i001p00023.
- Córdoba, D., E. Banda, and J. Ansorge (1987), The Hercynian crust in northwestern Spain, Tectonophysics, 132, 321-333.
- Dean, S. M., T. A. Minshull, R. B. Whitmarsh, and K. E. Louden (2000), Deep structure of the ocean-continent transition in the southern Iberia Abyssal Plain from seismic refraction profiles: The IAM-9 transect at 40º 20 ' N, Journal of Geophysical Research-Solid Earth, 105 (B3), 5859-5885.
- Derégnaucourt, D. & G. Boillot (1982) New structural map of the Bay of Biscay, Comptes Rendus De L´Academie Des Sciences de Paris Serie II, 294, 219-222, Paris.
- Ercilla, G., D. Casas, F. Estrada, J. T. Vazquez, J. Iglesias, M. Garcia, M. Gomez, J. Acosta, J. Gallart, A. Maestro-Gonzalez, and MARCONI Team (2008), Morphosedimentary features and recent depositional architectural model of the Cantabrian continental margin, Marine Geology, 247, 61-83, doi: 10.1016/j.margeo.2007.09.009.
- Espina, R. (1997), La estructura y evolución tectonoestratigráfica del borde occidental de la Cuenca Vasco-Cantábrica (Cordillera Cantábrica, NO de España), PhD thesis, Universidad de Oviedo, 230 pp.
- Fernández-Viejo, G., J. Gallart, J. A. Pulgar, J. Gallastegui, J. J. Dañobeitia, and D. Córdoba (1998), Crustal transition between continental and oceanic domains along the North Iberian margin from wide angle seismic and gravity data, Geophys. Res. Lett., 25, 4249-4252, doi: 10.1029/1998GL900149.
- Fernández-Viejo, G., J. Gallart, J. A. Pulgar, D. Córdoba, and J. J. Dañobeitia (2000), Seismic signature of Variscan and Alpine tectonics in NW Iberia: Crustal structure of the Cantabrian Mountains and Duero basin, J. Geophys. Res., B2, 3001-3018.
- Fernández-Viejo, G., J. Gallastegui, J. A. Pulgar, and J. Gallart (2011), The MARCONI reflection seismic data: A view into the eastern part of the Bay of Biscay, Tectonophysics, 508, 34-41, doi: 10.1016/j.tecto.2010.06.020.
- Fernández-Viejo, G., J.A. Pulgar, J. Gallastegui, and L. Quintana (2012), The Fossil Accretionary Wedge of the Bay of Biscay: Critical Wedge Analysis on Depth-Migrated Seismic Sections and Geodynamical Implications. J. Geol., 120 (3), 315-331, doi: 10.1086/664789.
- Fernández-Viejo, G., C. López-Fernández, M. J. Dominguez-Cuesta, and P. Cadenas (2014), How much confidence can be conferred on tectonic maps of continental shelves? The Cantabrian-Fault case, Scientific Reports, 4, 1-7, doi: 10.1038/srep03661.
- Ferrer, O., E. Roca, B. Benjumea, J. A. Muñoz, N. Ellouz, and MARCONI Team (2008), The deep seismic reflection MARCONI-3 profile: Role of extensional Mesozoic structure during the Pyrenean contractional deformation at the eastern part of the Bay of Biscay, Mar. Pet. Geol., 25, 714-730, doi: 10.1016/j.marpetgeo.2008.06.002.
- Fügenschuh, B., N. Froitzheim, R. Capdevila, and G. Boillot (2003), Offshore granulites from the Bay of Biscay margins: fission tracks constrain a Proterozoic to Tertiary thermal history.
- Gallart, J., E. Banda, and M. Daignières (1981), Crustal structure of the Paleozoic Axial Zone of the Pyrenees and transition to the North Pyrenean Zone, Ann. Geophys., 37, 457-480.
- Gallastegui, J. (2000) Estructura cortical de la cordillera y margen continental cantábricos: perfiles ESCI-N, Trabajos de Geología, 9-234, University of Oviedo, Oviedo.
- Gallastegui, J., J. A. Pulgar, and J. Gallart (2002), Initiation of an active margin at the North Iberian continent-ocean transition, Tectonics, 21,15-1-15-14, doi:10.1029/2001TC901046.

- García-Mondéjar, J., V. Pujalte, & S. Robles (1986), Características sedimentológicas, secuenciales y tectonoestratigráficas del Triásico de Cantabria y norte de Palencia, Cuadernos de Geología Ibérica, 10, 151-172.
- García-Mondéjar, J. (1996), Plate reconstruction of the Bay of Biscay, Geology, 24, 635-638.
- Gong, Z., C. G. Langereis, and T. A. T. Mullender (2008), The rotation of Iberia during the Aptian and the opening of the Bay of Biscay, Earth and Planetary Science Letters, 273, 80-93, doi: 10.1016/j.epsl.2008.06.016.
- González-Fernández, B., E. Menéndez-Casares, M. Gutiérrez-Claverol, and J.C. García-Ramos (2004) Litoestratigrafía del sector occidental de la cuenca cretácica de Asturias, Trabajos de Geología, 24, 43-80.
- González-Fernández, B., E. Menéndez-Casares, V. Vicedo, C. Aramburu, and E. Caus (2014), New insights about the Upper Jurassic-Lower Cretaceous sedimentary succesions from Asturias (NW Iberian Peninsula), Journal of Iberian Geology, 40,3, 409-430.
- Gutiérrez-Claverol, M. and J (2002), Prospección de hidrocarburos en la plataforma continental de Asturias, Trabajos de Geología, 23, 21-34, University of Oviedo, Oviedo.
- Huismans, R., and C. Beaumont (2011), Depth-dependent extension, two-stage breakup and cratonic underplating at rifted margins, Nature, 473, 74-78, doi: 10.1038/nature09988.
- Jabaloy, A., L. Galindo-Zaldívar, and F. González-Lodeiro (2002), Palaeostress evolution of the Iberian Peninsula (Late Carboniferous to present-day), Tectonophysics, 357, 159-186.
- Jammes, S., G. Manatschal, L. Lavier, and E. Masini (2009), Tectonosedimentary evolution related to extreme crustal thinning ahead of a propagating ocean: Example of the western Pyrenees, Tectonics, 28, TC4012, doi: 10.1029/2008TC002406.
- Jammes, S., C. Tiberi, and G. Manatschal (2010), 3D architecture of a complex transcurrent rift system: The example of the Bay of Biscay-Western Pyrenees, Tectonophysics, 489, 210-226, doi: 10.1016/j.tecto.2010.04.023.
- Julivert, M., Ramírez el Pozo, J., & Truyols, J. (1971), Le réseau des failles et la converture post-hercynienne dans les Asturies, in: Historie structurale du Golfe de Gascogne, edited by: J. Debysier, X. Le Pichon and M. Montadert, Technip, París, V. 6-V6.52.
- Kimbell, G. S., M. A. Stewart, S. Gradmann, P. M. Shannon, T. Funck, C. Haase, M. S. Stoker, and J. R. Hopper (2016), Controls on the location of compressional deformation on the NW European margin, in: The NE Atlantic Region: A Reappraisal of Crustal Structure, Tectonostratigraphy and Magmatic Evolution, Edited by G. Péron-Pinvidic et al., Geol. Soc. London Spec. Publ., pp. 447 doi: 10.1144/SP447.3.
- Lagabrielle, Y., P. Labaume, and M.Saint Blanquat (2010), Mantle exhumation, crustal denudation, and gravity tectonics during Cretaceous rifting in the Pyrenean realm (SW Europe): Insights from the geological setting of the Iherzolite bodies, Tectonics, 29, TC4012, doi: 10.1029/2009TC002588.
- Lanaja, J.M. (1987), Contribución de la exploración petrolífera al conocimiento de la geología de España, Instituto Geológico y Minero de España, Madrid.
- Larrasoaña, J.C., J.M. Parés, H. Millán, J. del Valle, and E.L. Pueyo (2003), Paleomagnetic, structural, and stratigraphic constraints on transverse fault kinematics during basin inversion: The Pamplona Fault (Pyrenees, north Spain), Tectonics, 22,6, 10-1,10-22.
- Laughton, A.S., *et al.*, (1972), Site 118, in Initial Reports of the Deep Sea Drilling Project Covering Leg 12 of the Cruises of the Drilling Vessel Glomar Challenger, Boston, Massachusetts to Lisbon, Portugal, vol. 12, edited by A.S. Laughton et al., pp. 673-751, Ocean Drilling Program, College Station, Tex.
- Lavier, L. L., and G. Manatschal (2006), A mechanism to thin the continental lithosphere at magma-poor margins. Nature, 440 (7082), 324-328, doi: 10.1038/nature04608.
- Lepvrier, C. and E. Martínez-García (1990), Fault development and stress evolution of the post-Hercynian Asturian Basin (Asturias and Cantabria, northwestern Spain), Tectonophysics, 184, 345-356.
- Lister, G. (1986) Detachment faulting and the evolution of passive continental margins, Geology, 14, 246-250.

- Lundin, E.R., and A. G. Doré (2011), Hyperextension, serpentinization, and weakening: A new paradigm for rifted margin compressional deformation, Geology, 39, 347-350, doi: 10.1130/G31499.1.
- Malod, J., G. Boillot, R. Capdevila, P.A. Dupeuble, C. Lepvrier, G. Mascle, and J. Taugourdeu-Lantz (1982), Subduction and tectonics on the continental margin off northern Spain; observations with the submersible Cyana, in: Trench-Fore Arc Geology, Edited by J. K. Legett, Geol. Soc. London Spec. Publ., 10, 309-315.
- Malod, J.A. and M. Mauffret (1990), Iberian plate motions during the Mesozoic, Tectonophysics, 184, 261-278, The Geological Society of London, London.
- Marcos, A. (1979), Facies differentiation caused by wrench deformation along a deep-seated fault system (León Line, Cantabrian Mountains, North Spain)-Discussion, Tectonophysics, 60, 303-309.
- Martínez-Álvarez, J.A. (1968), Consideraciones respecto a la zona de fractura ("Falla Cantábrica") que se desarrolla desde Avilés (Asturias) hasta Cervera del Pisuerga (Palencia), Acta Geológica Hispánica, t. III, 142-144.
- Martínez-Catalán, J.R., P. Ayarza, J.A. Pulgar, A. Pérez-Estaún, J. Gallart, A. Marcos, F. Bastida, J. Álvarez-Marrón, F. González-Lodeiro, J. Aller, J.J. Dañobeitia, E. Banda, D. Córdoba, and M.C. Comas (1995), Results from the ESCIN-N3.3 marine deep seismic profile along the Cantabrian continental margin, Rev. Soc. Geol. España, 8, 4,341-354.
- Martínez-García, E. (1981), Tectónica y mineralizaciones pérmicas en la Cordillera Cantábrica Oriental (Noroeste de España), Cuader. Lab. Xeol. Laxe, 2, 263-271, SGE-ITGME, Madrid.
- Martínez-García, E. (1983), El Pérmico de la Región Cantábrica, In: Carbonífero y Pérmico de España, Edited by: C. Martínez-García, Inst. Geol. Min. Esp., Madrid, 389-402.
- Martínez-García, E (2004) El Pérmico de Asturias, 268-269, In: Geología de España, Edited by: J.A. Vera, SGE-IGME.
- Masini, E., G. Manatschal, and G. Mohn (2013), The Alpine Tethys rifted margins: Reconciling old and new ideas to understand the stratigraphic architecture of magma-poor rifted margins, Sedimentology, 60, 174-196.
- Matte, P. (1991), Accretionary history and crustal evolution of the Variscan in Western Europe, Tectonophysics, 196, 309-337.
- Minshull, T. (2009), Geophysical characterisation of the ocean-continent transition at magma-poor rifted margins, C.R. Geosci., 341, 382-393.
- Mohn, G., G. Manatschal, M. Beltrando, E. Masini, and N. Kusznir (2012), Necking of continental crust in magma-poor rifted margins: Evidence from the fossil Alpine Tethys margins, Tectonics, 31, pp. 28, TC2012, doi: 10.1029/2011TC002961.
- Mohn, G., G. Manatschal, M. Beltrando, and I. Haupert (2014), The role of rift-inherited hyperextension in Alpine-type orogens, Terra Nova, 26, 347-353, doi: 10.1111/ter.12104.
- Mohn, G., G.D. Karner, G. Manatschal, and C.A. Johnson (2015), Structural and stratigraphic evolution of the Iberia-Newfoundland hyper-extended rifted margin: a quantitative modelling approach, In: Sedimentary Basins and Crustal Processes at Continental Margins: From Modern Hyper-extended Margins to Deformed Ancient Analogues, Edited by: G.M. Gibson et al., Geol. Soc. London, Spec. Publ., 413, doi: 10.1144/SP413.9.
- Montadert, L., B. Damotte, J.R. Delteil, P. Valery, and E. Winnock. (1971), Structure géologique de la marge continentale septentrionale du Golfe de Gascogne, In: Historie structurale du Golfe de Gascogne, Edited by J. Debysier, X. Le Pichon and M. Montadert, Technip, París, V. III.2-III.2-20.Mouthereau, F., P.Y. Filleaudeau, A. Vacherat, R. Pik, O. Lacombe, M.G. Fellin, S. Castelltort, F. Christophoul, and E. Masini. (2014), Placing limits to shortening evolution in the Pyrenees: role of margin architecture and implications for the Iberia/ Europe convergence, Tectonics, 33, doi: 10.1002/2014TC003663.
- Muñoz, J. A. (1992), Evolution of a continental collision belt: ECORS-Pyrenees crustal balanced section, in Thrust Tectonics, Edited by K. R. MacClay, 235-246, Chapman and Hall, London.
- Nirrengarten, M., G. Manatschal, X.P. Yuan, N.J. Kusznir, and B. Maillot (2016) Application of the critical Coulomb wedge theory to hyper-extended, magma-poor rifted margins, Earth and Planetary Sci. Let., 442,121-132, doi: 10.1016/j.epsl.2016.03.004.

- Nirrengarten, M., G. Manatschal, J. Tugend, N.J. Kusznir, and D. Sauter (2017), Nature and origin of the J-magnetic anomaly offshore Iberia-Newfoundland: implications for plate reconstructions, Terra Nova, 29, 20-28, doi: 10.1111/ter.12240.
- Osmundsen, P.T., and T. F. Redfield (2011), Crustal taper and topography at passive continental margins, Terra Nova 23, 349-361.
- Pedreira, D., J.A. Pulgar, J. Gallart, and J. Diaz (2003), Seismic evidence of Alpine crustal thickening and wedging from the western Pyrenees to the Cantabrian Mountains (north Iberia), J. Geophys. Res., 108, B42204, doi: 10.1029/2001JB001667.
- Pedreira, D., J. A. Pulgar, J. Gallart, and M. Torné (2007), Three-dimensional gravity and magnetic modeling of crustal indentation and wedging in the western Pyrenees-Cantabrian Mountains. J. Geophys. Res., 112, B12405, doi: 10.129/2007JB00521.
- Pedreira, D., J.C. Alfonso, J.A. Pulgar, J. Gallastegui, A. Carballo, M. Fernández, D. García-Castellanos, I. Jiménez-Munt, J. Semprich, and O. García-Moreno (2015) Geophysical-petrophysical modeling of the lithosphere beneath the Cantabrian Mountains and the North Iberian margin: geodynamic implications, Lithos, doi: 10.1016/j.lithos.2015.04.018.
- Pérez-Gussinyé, M., T. J. Reston, and P. Morgan (2001), Rheological evolution during extension at nonvolcanic rifted margins: Onset of serpentinization and development of detachments leading to continental breakup, J. Geophys. Res. Earth, 106, 3961-3975, doi: 10.1029/2000JB00325.
- Pérez-Gussinyé, M., C.R. Ranero, T.J. Reston, and D. Sawyer (2003), Mechanisms of extension at non-volcanic margins. Evidence from the Galicia interior basin, west of Iberia, J. Geophys. Res., 108 (B5), 2245, doi: 10.1029/2001JB000901.
- Péron-Pinvidic, G., G. Manatschal, S.M. Dean, and T.A. Minshull (2008), Compressional structures on the West Iberia rifted margin: controls on their distribution, in: The Nature and Origin of Compression in Passive Margins, Edited by H. Johnson et al., Geol. Soc. London Spec. Publ. 306, 169-183, The Geological Society of London, London.
- Péron-Pinvidic, G., Manatschal, G., Minshull, T.A., and Sawyer, D.S. (2007), Tectono-sedimentary evolution of the deep Iberia-Newfoundland margins: Evidence for a complex breakup history. Tectonics, 26, TC20011, doi: 10.1029/2006TC001970.
- Péron-Pinvidic, G., and G. Manatschal (2009), The final rifting evolution at deep magma-poor passive margins from Iberia-Newfoundland: a new point of view. International Journal of Earth Sciences 98, 1581-1597, doi: 10.1007/s00531-008-0337-9.
- Péron-Pinvidic, G. and G. Manatschal (2010) From microcontinents to extensional allochthons: witnesses of how continents rift and break apart?, Pet. Geosci., 16,189-197, doi: 10.1144/1354-079309-903.
- Péron-Pinvidic, G., G. Manatschal, and P. T. Osmundsen (2013), Structural comparison of archetypal Atlantic rifted margins: A review of observations and concepts, Marine and Petroleum Geology, 43, 21-47, doi: 10.1016/j.marpetgeo.2013.02.002.
- Pieren, A. P., J.L. Areces, J. Toraño, and E. Martínez-García (1995), Estratigrafía y estructura de los materiales permotriásicos del sector Gijón-La Collada (Asturias). Cuadernos de Geología Ibérica, 19, 309-335, Universidad Complutense de Madrid, Madrid.
- Pinet, B., L. Montadert, and ECORS Scientific Party (1987), Deep seismic reflection and refraction profiling along the Aquitaine shelf (Bay of Biscay), Geophys. J.R. astr.Soc., 89, 305-312.
- Pitman, W. and M. Talwani (1972), Sea-Floor Spreading in the North Atlantic, Geol. Soc. Amer. Bul., 83, 619-646.
- Pulgar, J., J. Gallart, G. Fernández-Viejo, A. Pérez-Estaún, J. Álvarez-Marrón, and ESCIN Group (1996), Seismic image of the Cantabrian Mountains in the western extension of the Pyrenees from integrated ESCIN reflection and refraction data, Tectonophysics, 264, 1-19.
- Pulgar, J.A., J.L. Alonso, R.G. Espina, and J.A. Marín (1999), La deformación alpina en el basamento varisco de la Zona Cantábrica, Trabajos de Geología, Univ. Oviedo, 21,283-294.
- Quintana, L. (2012), Extensión e inversión tectónica en el sector central de la Región Vasco-Cantábrica, PhD Thesis, pp. 560, University of Oviedo, Department of Geology.

- Quintana, L., J. A. Pulgar, and J. L. Alonso (2015), Displacement transfer from borders to interior of a plate: A crustal transect of Iberia, Tectonophysics, 663, 378-398, doi: 10.1016/j.tecto.2015.08.046.
- Riaza, C. (1996) Inversión estructural en la cuenca mesozoica del off-shore asturiano. Revisión de un modelo exploratorio, Geogaceta, 20 (1), 169-171.
- Robles, S. and V. Pujalte (2004) El Triásico de la Cordillera Cantábrica, In: Geología de España, Edited by: J.A. Vera, SGE-IGME, 274-275.
- Roca, E., J.A. Munoz, O. Ferrer, and N. Ellouz (2011), The role of the Bay of Biscay Mesozoic extensional structure in the configuration of the Pyrenean orogen: Constraints from the MARCONI deep seismic reflection survey, Tectonics, 30, TC2001, doi: 10.1029/2010TC002735.
- Roest, W.R., and S. P. Srivastava (1991), Kinematics of the plate boundaries between Eurasia, Iberia and Africa in the North-Atlantic from the Late Cretaceous to the present, Geology, 19, 613-616, doi: 10.1130/0091-7613.
- Rosenbaum, G., G. S. Lister, and C. Duboz (2002) Relative motions of Africa, Iberia and Europe during Alpine orogeny, Tectonophysics, 359, 117-129.
- Ruiz, M. (2007), Caracterització structural I sismotectònica de la litosfera en el domini Pirenaico-Cantàbric a partir de mètodes de sísmica active I passive. PhD Thesis, 354 pp, Univ. of Barcelona, Barcelona.
- Salas, R. and A. Casas (1993), Mesozoic extensional tectonics stratigraphy and crustal evolution during the Alpine cycle of the eastern Iberian basin, Tectonophysics, 228, 33-55, doi: 10.1016/0040 -1951 (93) 90213-4.
- Salas, R., J. Guimerà, R. Mas, C. Martín-Closas, A. Meléndez, and A. Alonso (2001), Evolution of the Mesozoic Central Iberian Rift System and its Cainozoic inversion (Iberian chain), in: Peri-Tethys Memoir 6: Peri-Tethyan Rift/Wrench Basins and Passive Margins, edited by: P.A. Ziegler, W. Cavazza, A.H.F. Robertson and S. Crasquin-Soleau, Mém. Mus. Nast. Hist. nat., 186, 145-185, Paris, ISBN: 2-85653-528-3.
- Sibuet, J. C., and B. J. Collette (1991), Triple junctions of Bay of Biscay and North Atlantic: New constraints on the kinematics evolution, Geology, 19, 522-525.
- Sibuet, J.C., S.P. Srivastava, and W. Spakman (2004), Pyrenean orogeny and plate kinematics. J. Geophys. Res. 109, B08104, doi: 10.1029/2003JB002514.
- Sibuet, J.C., S. Srivastava, and G. Manatschal (2007), Exhumed mantle-forming transitional crust in the Newfoundland-Iberia rift and associated magnetic anomalies. J. Geophys. Res., 112, B06105, doi: 10.1029/2005JB003856.
- Srivastava, S. P., W. R. Roest, L. C. Kovacs, G. Oakey, S. Lévesque, J. Verhoef, and R. Macnab (1990), Motion of Iberia since the Late Jurassic: results form detailed aeromagnetic measurements in the Newfoundland basin, Tectonophysics, 184, 229-260.
- Srivastava, S.P., J.C., Sibuet, S. Cande, W.R. Roest, and I.D. Reid (2000), Magnetic evidence for slow seafloor spreading during the formation of the Newfoundland and Iberian margins, Earth and Planetary Science Letters, 182, 61-76, doi: 10.1016/S0012-821X (00)00231-4.
- Suárez-Rodríguez, A. (1988), Estructura del área de Villaviciosa-Libardón (Asturias, Cordillera Cantábrica), Trabajos de Geología, 17,87-98.
- Sutra, E., G. Manatschal, G. Mohn, and P. Unternehr (2013), Quantification and restoration of extensional deformation along the Western Iberia and Newfoundland rifted margins, Geochem. Geophys. Geosyst., 14, 2575-2597, doi: 10.1002/ggge.20135.
- Teixell, A. (1998), Crustal structure and orogenic material budget in the west central Pyrenees, Tectonics, 17, 395-406, doi: 10.1029/98TC00561.
- Teixell, A, P. Labaume, P., and Y. Lagabrielle (2016), The crustal evolution of the west-central Pyrenees revisited: Inferences from a new kinematic scenario, C.R. Geosci., 348, 257-267.
- Tejerina, L. and I. Vargas (1980), Descripción geológica del distrito minero de La Collada (Fluorita teletermal) Asturias, Tecniterrae, S-246, 44-53.
- Tellez, J. (1993), Análisis e interpretación de ondas P y S de perfiles sísmicos: aplicación al NO de la Península Ibérica, PhD Thesis, pp. 309, Universidad Complutense de Madrid.

- Thinon, I., L. Fidalgo-González, J. P. Réhault, and J. L. Olivet (2001), Déformations pyrénéennes dans le golfe de Gascogne. C.R. Acad. Sci. Paris, Ser. IIa: Sci. Terre Planets, 332, 561-568, Academie des Sciences de Paris, Paris.
- Thinon, I., J.P. Réhault, and L. Fidalgo-González (2002), The syn-rift sedimentary cover of the North Biscay Margin (bay of Biscay): From new reflection seismic data, Bull. Soc. Geol. Fr., 173, 515–522.
- Thinon, I., L. Matias, J. P. Réhault, A. Hirn, L. Fidalgo-Gonzalez, and F. Avedik (2003), Deep structure of the Armorican Basin (Bay of Biscay): a review of Norgasis seismic reflection and refraction data, J. Geol. Soc., 160, 99-116.
- Tucholke, B.E., D. Sawyer, and J. C. Sibuet (2007), Breakup of the Newfoundland-Iberia rift, In: G. D. Karner, G. Manatschal and L. M. Pinheiro (Eds.),Imaging, Mapping and Modelling Continental Lithosphere Extension and Breakup, Geol. Soc. London Spec. Publ., 282, 9-46, The Geological Society of London, London.
- Tugend, J., G. Manatschal, N.J. Kusznir, E. Masini, G. Mohn, and I. Thinon (2014), Formation and deformation of hyperextended rift systems: Insights from rift domain mapping in the Bay of Biscay-Pyrenees, Tectonics, 33, 1239-1276, doi: 10.1002/ 2014TC003529.
- Tugend, J., G. Manatschal, N. J. Kusznir, and E. Masini (2015a), Characterizing and identifying structural domains at rifted continental margins: application to the Bay of Biscay margins and its Western Pyrenean fossil remnants. In: Sedimentary Basins and Crustal Processes at Continental Margins: From Modern Hyper-extended Margins to Deformed Ancient Analogues, Edited by: G.M. Gibson et al., Geol. Soc. London, Spec. Publ., 413, 171-203, doi: 10.1144/SP413.3, The Geological Society of London, London.
- Tugend, J., G. Manatschal and N.J. Kusznir (2015b), Spatial and temporal evolution of hyperextended rift systems: Implication for the nature, kinematics, and timing of the Iberian-European plate boundary, Geology, 43 (1), 15-18, doi: 10.1130/G36072.
- Uzkeda, H., M. Bulnes, J. Poblet, J.C. García-Ramos, and L. Piñuela (2016), Jurassic extension and Cenozoic inversion tectonics in the Asturian Basin, NW Iberian Peninsula: 3D structural model and kinematic evolution, Journal of Structural Geology, 90, 157-176.
- Valenzuela, M, J.C. García-Ramos, and C. Suárez de Centi (1986), The Jurassic sedimentation in Asturias (N Spain), Trabajos de Geología, 16, 121-132.
- Vergés, J., H. Millán, E. Roca, J.A. Muñoz, and M. Marzo (1995) Eastern Pyrenees and related foreland basins: pre-, syn- and post-collisional crustal-scale cross-sections, Mar. Pet. Geol., 12 (8), 893-915,
- Vergés, J., M. Fernández, and A. Martínez (2000), The Pyrenean orogen: pre-, syn-, and post-collisional evolution, In: G. Rosembaum & G. S. Lister (Eds.), Reconstruction of the evolution of the Alpine-Himalayan Orogen, Journal of the Virtual Explorer, 8, 55-74.
- Vergés, J. and J. García-Senz (2001) Mesozoic evolution and Cainozoic inversion of the Pyrenean Rift, In: Peri-Tethys Memoir 6: Peri-Tethyan Rift/ Wrench Basins and Passive Margins, Edited by P.A. Ziegler et al., Mém. Mus. natn. Hist. nat., 186, 187-212, ISBN: 2-85653-528-3.
- Virgili, C., L.C. Suárez-Vega, and R. Rincón (1971), Le Mésozoique des Asturies (Nord de l´Espagne), in: Historie structurale du Golfe de Gascogne, edited by J. Debysier, X. Le Pichon and M. Montadert, Technip, París, V. 4-V4.20.
- Vissers, R.L.M., and P. T. Meijer (2012), Mesozoic rotation of Iberia: Subduction in the Pyrenees? Earth Sci. Rev., 110, 93-110, doi: 10.1016/j.earscirev.2011.11.001.
- Wagner, R.H. and E. Martínez-García (1982) Description of an early Permian flora from Asturias and comments on similar occurrences in the Iberian península, Trabajos de Geología, 12, 273-287, University of Oviedo, Oviedo.
- Zamora, G., M. Fleming, and J. Gallastegui (2017) Salt Tectonics within the offshore Asturian Basin: North Iberian margin, In: J.I. Soto, J.F. Flinch & G. Tari (Eds.), Permo-Triassic salt provinces of Europe, North Africa and the Atlantic Margins, Chapter 16, 358-368, Elsevier.
- Ziegler P.A. (1988), Evolution of the Artic-North Atlantic and the Western Tethys, AAPG Memoir, 43, 198 pp, American Association of Petroleum Geologists.

• Ziegler, P.A. & P. Dèzes (2006), Crustal evolution of Western and Central Europe. In: European Lithosphere Dynamics, Edited by D.G. Gee and R.A. Stephenson, Geol. Soc. Mem, London, 32, 43-56.

FIGURE CAPTIONS

Figure 1. First-order architecture of a hyperextended magma-poor rifted margin; **a)** Idealized cross section showing the main features of rift domains from continent to ocean, following the terminology proposed by *Tugend et al.* [2015a]; **b)** Crustal structure, stratigraphic architecture, type of basement and major structures characterizing the proximal, the necking and the hyperthinned domains (from *Péron-Pinvidic et al.* [2013].

Figure 2. Geological context of the studied zone; **a)** Location map of the studied area within the context of the Bay of Biscay and the Pyrenean-Cantabrian orogen, displaying the distribution of the dataset used. Based on *Alonso et al.* [1996], *Fernández-Viejo et al.* [2012], *Roca et al.* [2011], *Thinon et al.* [2001] and *Tugend et al.* [2014]. The white dashed rectangle delineates the studied zone. Magnetic anomalies are from *Sibuet et al.* [2004]. Mesozoic basins: **AB**: Asturian Basin, **BCB:** Basque-Cantabrian Basin; **PB**: Parentis Basin, **AMB**: Armorican Basin. Structures: **STZ**: Santander Transfer Zone. The black rectangle delineates the area displayed in detail in b; **b)** Structure and distribution of the Mesozoic outcrops in the Cantabrian Mountains. After *Cadenas & Fernández-Viejo* [2018] and *Pulgar et al.* [1999].

Figure 3. Representative time migrated seismic reflection lines crossing the North Iberian margin at three different longitudes, showing the seismic interpretation of the main structures, the first order interfaces and, on top, the interpreted rift domains. **A)** CS01-108 seismic line at the westernmost area; **B)** CS01-133 section at the central part of the margin **C)** CS01-142 seismic profile located in the easternmost part of the studied zone. The seismic Moho and the presence of anomalous mantle velocities (V_p < 8 km/s) have been estimated using the velocity models of *Ayarza et al.* [1998], *Fernández-Viejo et al.* [1998, 2012], and *Ruiz* [2007]. The inset map shows the location of the reflections lines within the seismic dataset (red). The map also displays the Moho depth and the distribution of the wide-angle profiles used to estimate its position. IAM-12 profile, displayed in pink, ESCIN-3.1, shown in green, and ESCIN-4, delineated with a dashed black line, are from *Fernández-Viejo et al.* [1998]; ESCIN-3.3, displayed in black, is from *Ayarza et al.* [1998]; MARCONI profiles, shown in yellow (MARCONI-1 and MARCONI-6 from west to east, and MARCONI-4 and MARCONI-8 from north to south) are from *Ruiz* [2007]. **CF**: Cantabrian fault from *Fernández-Viejo et al.* [2014]. F1 to F5 faults in the Asturian Basin from *Cadenas* & *Fernández-Viejo* [2017]. The uninterpreted version of the three seismic profiles is provided as supplementary information (Figure S1).

Figure 4. CS01-132 depth migrated seismic reflection profile. The seismic line runs from the Cantabrian Platform to the Biscay Abyssal Plain, crossing the central part of the Asturian Basin and the Le Danois High. The figure shows the seismic interpretation of the main structures and the first-order interfaces, illustrating the crustal architecture, and the interpreted rift domains on top. A column with the migration velocities is shown at the left, with the depths of the main interpreted surfaces. **SF**: seafloor; **TSB**: top seismic basement; **RF**: refraction Moho. The vertical line between SP 900 and 1000 shows the profile where the velocity column has been extracted. The inset shows the location of the depth migrated profile and the wide-angle sections used to estimate the Moho depth. ESCIN-4 from *Fernández-Viejo et al.* [1998]; MARCONI-1 from *Ruiz* [2007].

Figure 5. Enlargements of three seismic profiles showing the stratigraphic architecture of the main structural areas identified within the central and western North Iberian margin. Exaggerated vertical scale; **a)** Line CS01-107, displaying the structure of the rift basin identified in the westernmost continental platform; **b)** Profile CS01-133, showing the main structures and seismic sequences identified within the central part of the Asturian Basin; **c)** Line CS01-132, in the central North Iberian margin, displaying the structure of the accretionary wedge developed in the abyssal plain (modified from *Cadenas & Fernández-Viejo* [2017]). Age of the pre-orogenic, the syn-orogenic and

the post-orogenic deposits from *Álvarez-Marrón et al.* [1997] and *Fernández-Viejo et al.* [2011]. The uninterpreted version of the seismic profiles is provided as supporting information (Figure S2).

Figure 6. Lithologies, time constraints, and tectono-stratigraphic correlations along four representative boreholes drilled within the platform around the studied zone. The definition of the tectono-stratigraphic units has been developed using seismic to well ties from which we assigned ages to the interpreted seismic units. Borehole **Galicia-B2**, representative of the proximal domain, **Mar Cantábrico K1**, representative of the necking area, and **Mar Cantábrico H1X** and **Mar Cantábrico M1** showing the thick sequences from the hyperthinned domain; **Mi**: Miocene; **Ol**: Oligocene; **Eo**: Eocene; **Pal**: Paleocene; **Ce**: Cenomanian; **Al**: Albian; **Ap**: Aptian; **Ba**: Barremian; **Ht**: Hauterivian; **Va**: Valanginian; **Be**: Berrasian; **Ki**: Kimmeridgian; **Neoco**: Neocomian; **Pu**: Purberk; **Li**: Lias; **Ra**: Raethian; **He**: Hettangian; **Ke**: Keuper; **Mu**: Muschelkalk; **Ca**: Carboniferous; **Tr**: Triassic; **Pa**: Palaeozoic.

Figure 7. 3D view of nine representative boreholes drilled in the Asturian Basin showing thickness variations of the main tectono-stratigraphic units along the whole area. The original stratigraphic information has been taken from the well reports. See *Cadenas & Fernández-Viejo* [2017], *Gutiérrez-Claverol* & *Gallastegui* [2002] and *Lanaja* [2007] for stratigraphic columns. We defined the main seismo-stratigraphic units displayed along the boreholes based on seismic to well ties. This figure is provided on a larger scale as supporting information (Figure S3).

Figure 8. Crustal thickness and main faults in the central and western North Iberian margin. **a)** Map of isolines resulting from subtracting the sediment thickness from the actual crustal thickness, based on the depth converted first-order interfaces interpreted in this study (Residual Crustal Thickness, RCT). F1, F2, F3 and F4 faults from *Cadenas* & *Fernández-Viejo* [2017]. Offshore trace of the Ventaniella fault from *Fernández-Viejo et al.* [2014]. Yellow points represent locations where granulites have been recovered (*Capdevila et al.* [1980]; *Fügenschuh et al.* [2003]; *Malod et al.* [1982]). The map shows the location of the sections displayed in b and c. **b)** Section illustrating crustal thickness variations in the western North Iberian margin along the CS01-107 seismic profile; **c)** Section showing crustal thickness variations in the central North Iberian margin along the CS01-132 seismic line; **d)** Rift domains boundaries superimposed on the Residual Crustal Thickness map. The RCT map shows more clearly, once the sediments are subtracted, the boundaries of the rift domains, bearing in mind that in some areas, the crust has been thickened during the Alpine compression.

Figure 9. Sediment thickness within the central and western North Iberian margin; **a)** Map of isolines showing thickness variations of the sedimentary cover, based on the depth converted first-order interfaces interpreted in this study. The map shows the location of the sections displayed in figure b and c; **b)** Section illustrating sediment thickness variations in the western North Iberian margin along the CS01-107 seismic profile; **c)** Section showing sediment thickness variations in the central North Iberian margin along the CS01-132 seismic line.

Figure 10. Isopachs map of the crust-mantle boundary onshore showing the Moho depth along the Cantabrian Mountains based on published refraction/wide angle reflection profiles. The dots reflect the segments of the profiles where good control by PmP /Pn phases was achieved in the refraction models. We used these segments to map the crust-mantle boundary displayed in the figure. The inset shows the distribution of the velocity models from which the Moho was gridded and contoured. Galicia survey lines delineated with dashed black lines from *Córdoba et al.* [1987] and *Tellez* [1993]; ESCIN-3.1 and ESCIN-4 profiles, IAM-12 section, and Profiles 1-5 are from *Fernández-Viejo et al.* [1998, 2000]; Profiles 1 and 6 from *Pedreira et al.* [2003]; and MARCONI-1 section from *Ruiz* [2007]. **CMF**: Cantabrian Mountains Front from *Alonso et al.* [1996]. **SPF**: South Pyrenean Front.

Figure 11. Detailed map of the rift domains in the inverted hyperextended North Iberian margin and in the western Cantabrian Mountains, after this study. **CMF**: Cantabrian Mountains Front (from *Alonso et al.* [1996]); **BWF**: Biscay Wedge Front (from *Fernández-Viejo et al.* [2012]). Offshore trace of Ventaniella fault from *Fernández-Viejo et al.* [2014]. **STZ**: Santander Transfer zone from *Roca et al.* [2011].

Figure 12. Rift domains map of the complete Bay of Biscay-Pyrenean system including the results of this work. Rift domains in the Basque-Pyrenean rift system and in the northern Biscay margin from *Tugend et al.* [2014, 2015b]. Oceanic magnetic anomalies and abbreviations are as in Figure 2. The dashed red square represents the area redefined in this study, which is displayed in detail in Figure 11.]. **Peñas TZ**: Peñas Transfer Zone, after *Cadenas* [2017]. **Santander TZ**: Santander Transfer Zone from *Roca et al.* [2011. Mesozoic basins within the Bay of Biscay rift: **AB**: Asturian Basin; **AMB**: Armorican Basin; **PB**: Parentis Basin. **CMF**: Cantabrian Mountains Front; **BWF**: Biscay Wedge Front: Biscay Wedge Front; **NP**F: North Pyrenean Front; **SPF**: South Pyrenean Front.

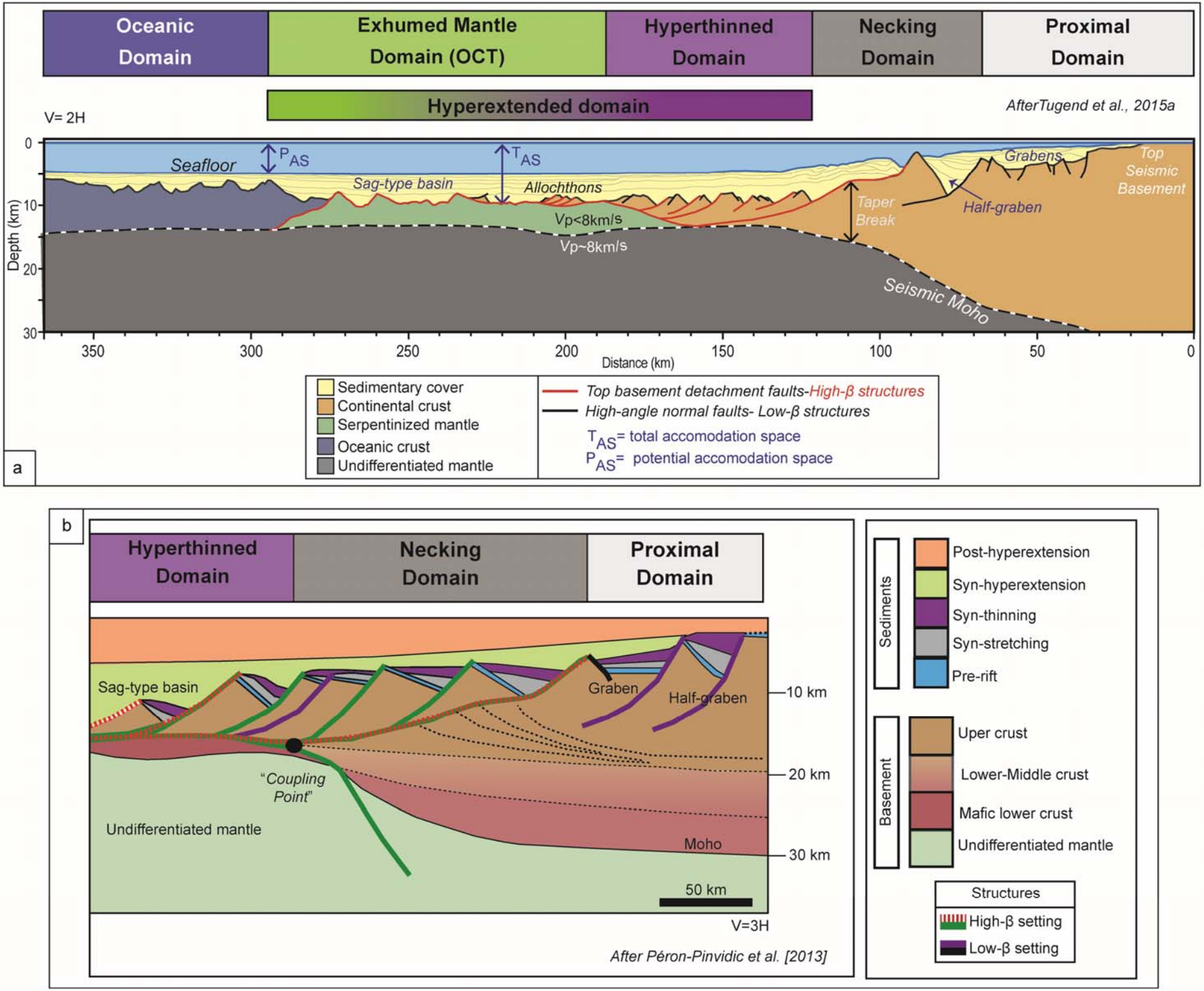
Oceanic Domain
Exhumed Mantle Domain (OCT)
Hyperthinned Domain
Necking Domain
Proximal Domain
Hyperextended domain
AfterTugend et al., 2015a
V= 2H
Seafloor
P_{AS}
T_{AS}
Sag-type basin
Allochthons
Vp<8km/s
Vp~8km/s
Taper Break
Grabens
Half-graben
Top Seismic Basement
Seismic Moho
Depth (km)
Distance (km)
Sedimentary cover
Continental crust
Serpentinized mantle
Oceanic crust
Undifferentiated mantle
Top basement detachment faults-High-β structures
High-angle normal faults- Low-β structures
T_{AS}= total accomodation space
P_{AS}= potential accomodation space
a
b
Hyperthinned Domain
Necking Domain
Proximal Domain
Sag-type basin
Graben
Half-graben
"Coupling Point"
Undifferentiated mantle
Moho
10 km
20 km
30 km
50 km
V=3H
After Péron-Pinvidic et al. [2013]
Sediments
Post-hyperextension
Syn-hyperextension
Syn-thinning
Syn-stretching
Pre-rift
Basement
Uper crust
Lower-Middle crust
Mafic lower crust
Undifferentiated mantle
Structures
High-β setting
Low-β setting

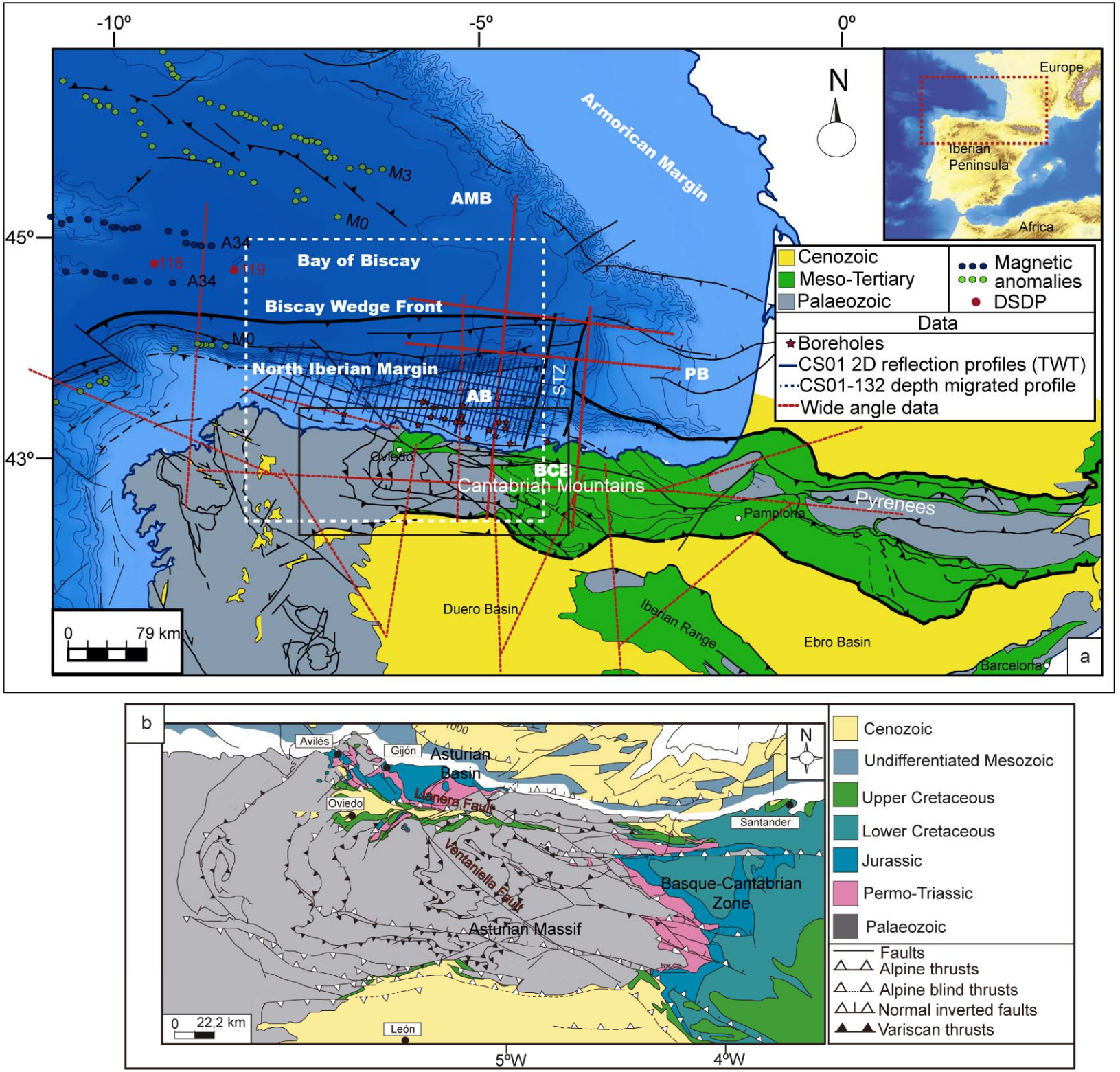
-10º
-5º
0º
45º
43º
N
Armorican Margin
AMB
M3
M0
A34
118
119
A34
Bay of Biscay
Biscay Wedge Front
M0
North Iberian Margin
AB
STZ
PB
BCB
Oviedo
Cantabrian Mountains
Pyrenees
Pamplona
Duero Basin
Iberian Range
Ebro Basin
Barcelona
0 79 km
a
Europe
Iberian Peninsula
Africa
Cenozoic
Meso-Tertiary
Palaeozoic
Magnetic anomalies
DSDP
Data
Boreholes
CS01 2D reflection profiles (TWT)
CS01-132 depth migrated profile
Wide angle data
b
Avilés
Gijón
Asturian Basin
Oviedo
Llanera Fault
Ventaniella Fault
Santander
Basque-Cantabrian Zone
Asturian Massif
León
0 22,2 km
5ºW
4ºW
Cenozoic
Undifferentiated Mesozoic
Upper Cretaceous
Lower Cretaceous
Jurassic
Permo-Triassic
Palaeozoic
Faults
Alpine thrusts
Alpine blind thrusts
Normal inverted faults
Variscan thrusts

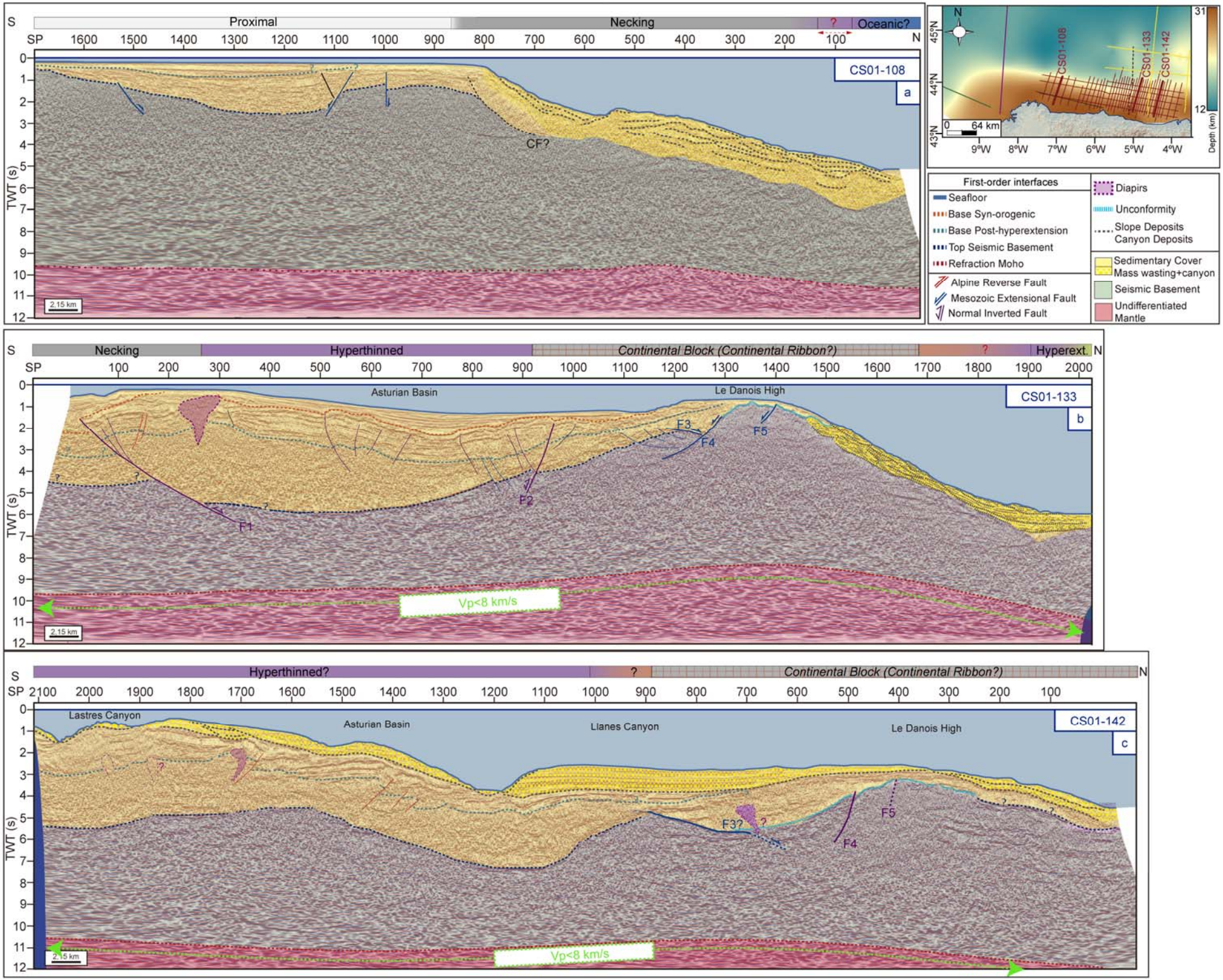
S
Proximal
Necking
?
Oceanic?
N
SP
1600 1500 1400 1300 1200 1100 1000 900 800 700 600 500 400 300 200 100
TWT (s)
CS01-108
a
CF?
2.15 km
N
45°N
44°N
43°N
CS01-108
CS01-133
CS01-142
0
64 km
9°W 8°W 7°W 6°W 5°W 4°W
31
12
Depth (km)
First-order interfaces
Seafloor
Base Syn-orogenic
Base Post-hyperextension
Top Seismic Basement
Refraction Moho
Alpine Reverse Fault
Mesozoic Extensional Fault
Normal Inverted Fault
Diapirs
Unconformity
Slope Deposits
Canyon Deposits
Sedimentary Cover
Mass wasting+canyon
Seismic Basement
Undifferentiated Mantle
S
Necking
Hyperthinned
Continental Block (Continental Ribbon?)
?
Hyperext.
N
SP
100 200 300 400 500 600 700 800 900 1000 1100 1200 1300 1400 1500 1600 1700 1800 1900 2000
Asturian Basin
Le Danois High
CS01-133
b
F1
F2
F3
F4
F5
Vp<8 km/s
TWT (s)
2.15 km
S
Hyperthinned?
?
Continental Block (Continental Ribbon?)
N
SP
2100 2000 1900 1800 1700 1600 1500 1400 1300 1200 1100 1000 900 800 700 600 500 400 300 200 100
Lastres Canyon
Asturian Basin
Llanes Canyon
Le Danois High
CS01-142
c
F3?
F4
F5
Vp<8 km/s
TWT (s)
2.15 km

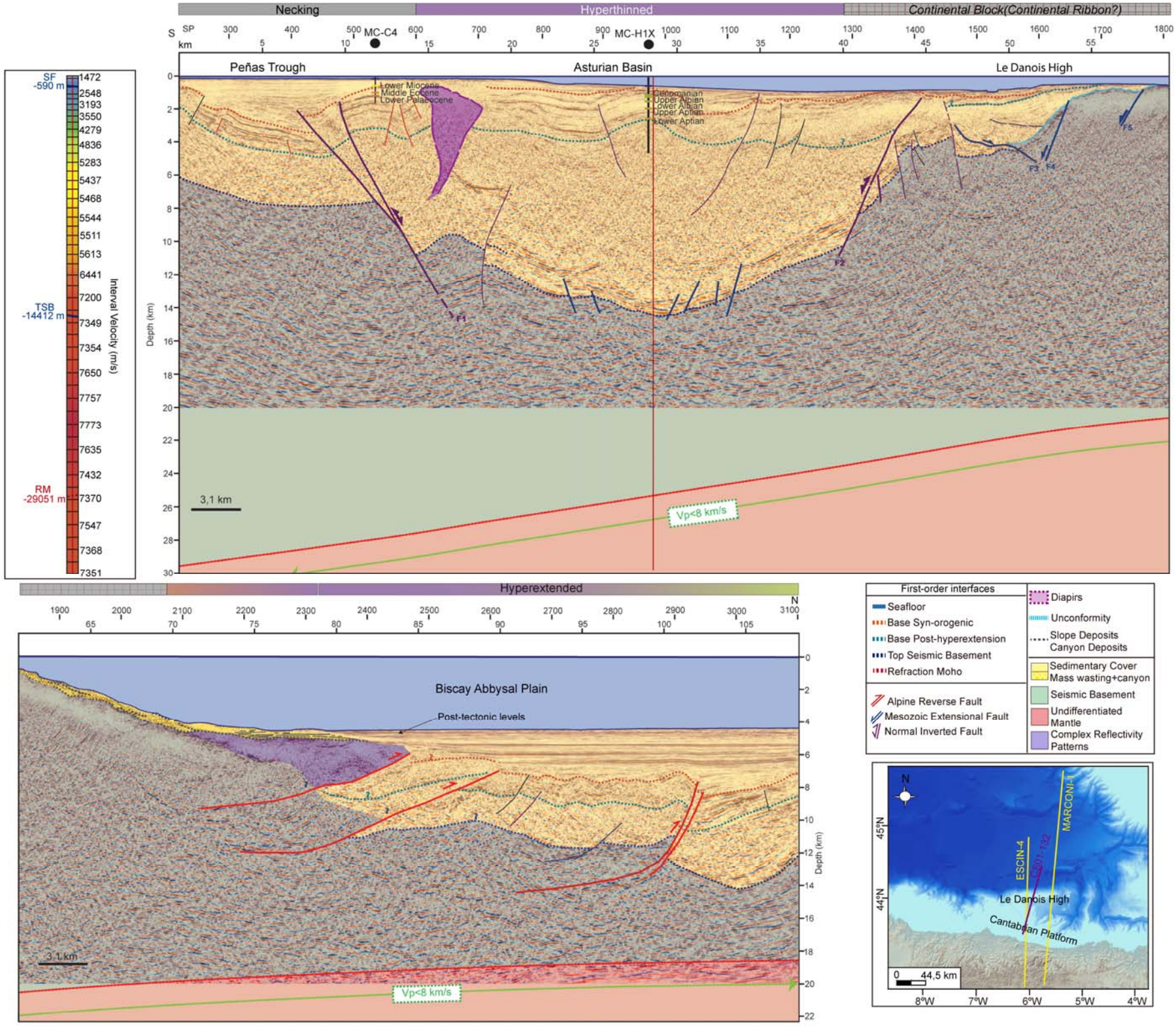
Necking
Hyperthinned
Continental Block(Continental Ribbon?)
S
SP
km
MC-C4
MC-H1X
N
Peñas Trough
Asturian Basin
Le Danois High
Lower Miocene
Middle Eocene
Lower Palaeocene
Cenomanian
Upper Albian
Lower Albian
Upper Aptian
Lower Aptian
F1
F2
F3
F4
F5
Depth (km)
3,1 km
Vp<8 km/s
SF
-590 m
TSB
-14412 m
RM
-29051 m
Interval Velocity (m/s)
1472
2548
3193
3550
4279
4836
5283
5437
5468
5544
5511
5613
6441
7200
7349
7354
7650
7757
7773
7635
7432
7370
7547
7368
7351
Hyperextended
Biscay Abbysal Plain
Post-tectonic levels
First-order interfaces
Seafloor
Base Syn-orogenic
Base Post-hyperextension
Top Seismic Basement
Refraction Moho
Alpine Reverse Fault
Mesozoic Extensional Fault
Normal Inverted Fault
Diapirs
Unconformity
Slope Deposits
Canyon Deposits
Sedimentary Cover
Mass wasting+canyon
Seismic Basement
Undifferentiated Mantle
Complex Reflectivity Patterns
MARCONI-1
ESCIN-4
SO91-132
Le Danois High
Cantabrian Platform
45°N
44°N
8°W
7°W
6°W
5°W
4°W
0
44,5 km

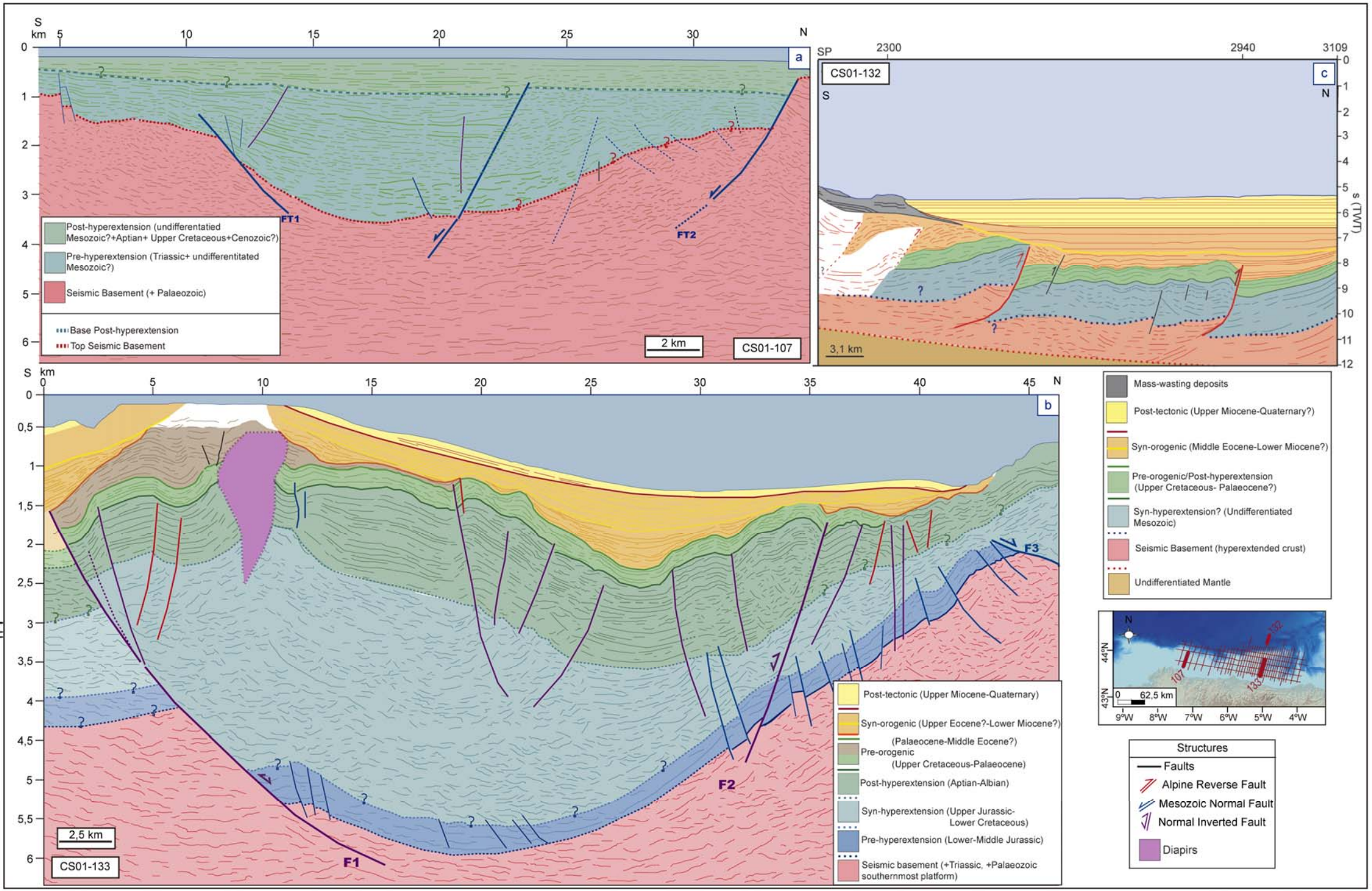
S
km
5
10
15
20
25
30
N
a
FT1
FT2
Post-hyperextension (undifferentatied Mesozoic?+Aptian+ Upper Cretaceous+Cenozoic?)
Pre-hyperextension (Triassic+ undifferentitated Mesozoic?)
Seismic Basement (+ Palaeozoic)
Base Post-hyperextension
Top Seismic Basement
2 km
CS01-107
SP
2300
2940
3109
CS01-132
c
S
N
3,1 km
s (TWT)
S km
0
5
10
15
20
25
30
35
40
45
N
b
F1
F2
F3
2,5 km
CS01-133
Post-tectonic (Upper Miocene-Quaternary)
Syn-orogenic (Upper Eocene?-Lower Miocene?)
(Palaeocene-Middle Eocene?)
Pre-orogenic
(Upper Cretaceous-Palaeocene)
Post-hyperextension (Aptian-Albian)
Syn-hyperextension (Upper Jurassic-Lower Cretaceous)
Pre-hyperextension (Lower-Middle Jurassic)
Seismic basement (+Triassic, +Palaeozoic southernmost platform)
Mass-wasting deposits
Post-tectonic (Upper Miocene-Quaternary?)
Syn-orogenic (Middle Eocene-Lower Miocene?)
Pre-orogenic/Post-hyperextension (Upper Cretaceous- Palaeocene?)
Syn-hyperextension? (Undifferentiated Mesozoic)
Seismic Basement (hyperextended crust)
Undifferentiated Mantle
N
44°N
43°N
107
132
133
0
62,5 km
9°W
8°W
7°W
6°W
5°W
4°W
Structures
Faults
Alpine Reverse Fault
Mesozoic Normal Fault
Normal Inverted Fault
Diapirs

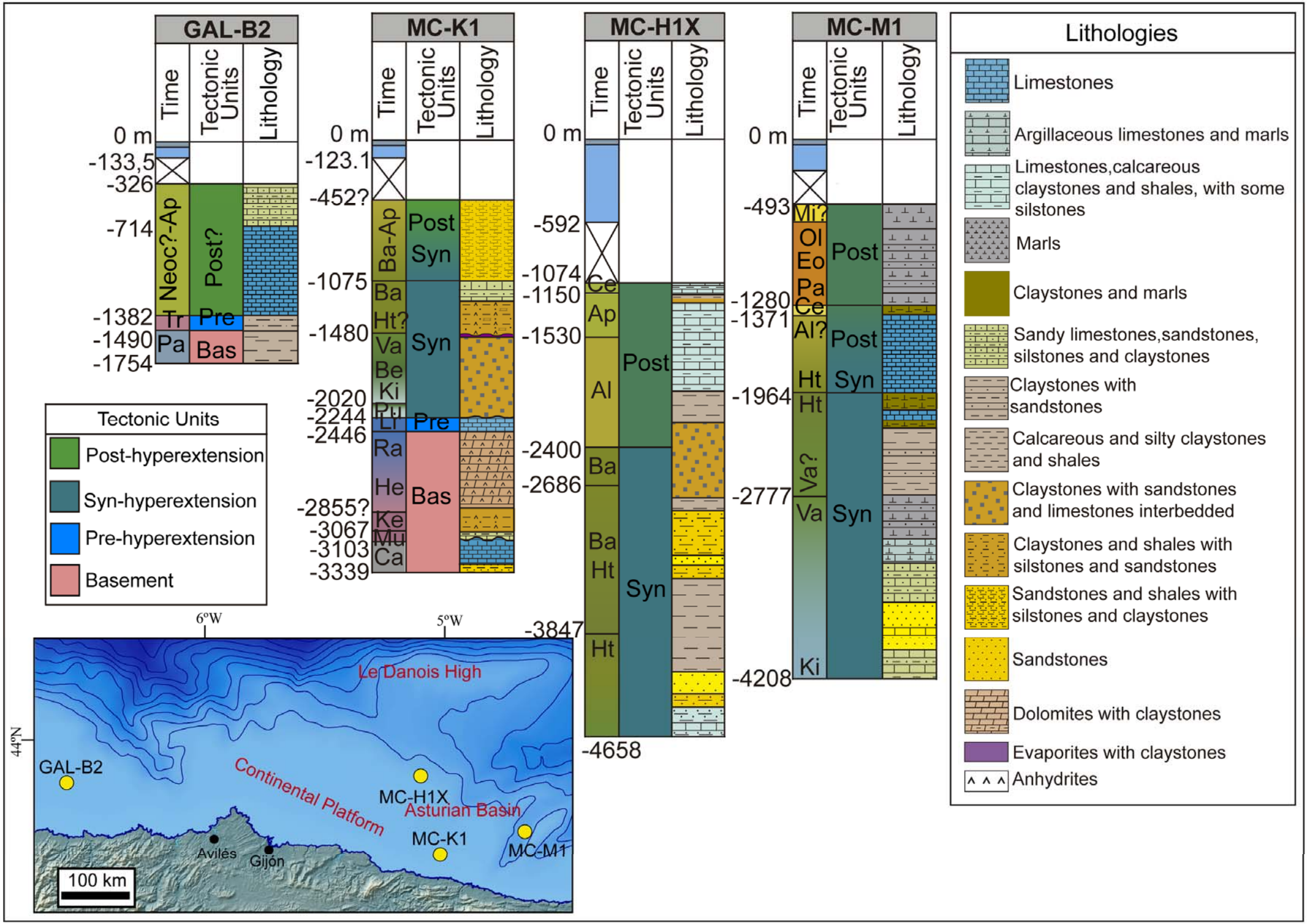
GAL-B2
MC-K1
MC-H1X
MC-M1
Time
Tectonic Units
Lithology
0 m
-133,5
-326
-714
-1382
-1490
-1754
Neoc?-Ap
Post?
Tr
Pre
Pa
Bas
-123.1
-452?
Ba-Ap
Post
Syn
-1075
Ba
Ht?
-1480
Va
Be
Ki
Syn
-2020
-2244
-2446
Pu
Li
Pre
Ra
He
Bas
-2855?
-3067
-3103
-3339
Ke
Mu
Ca
-592
-1074
-1150
-1530
-2400
-2686
-3847
-4658
Ce
Ap
Al
Ba
Ht
Post
Syn
-493
-1280
-1371
-1964
-2777
-4208
Mi?
Ol
Eo
Pa
Ce
Al?
Ht
Va?
Va
Ki
Tectonic Units
Post-hyperextension
Syn-hyperextension
Pre-hyperextension
Basement
6°W
5°W
44°N
Le Danois High
Continental Platform
Asturian Basin
GAL-B2
MC-H1X
MC-K1
MC-M1
Avilés
Gijón
100 km
Lithologies
Limestones
Argillaceous limestones and marls
Limestones,calcareous claystones and shales, with some silstones
Marls
Claystones and marls
Sandy limestones,sandstones, silstones and claystones
Claystones with sandstones
Calcareous and silty claystones and shales
Claystones with sandstones and limestones interbedded
Claystones and shales with silstones and sandstones
Sandstones and shales with silstones and claystones
Sandstones
Dolomites with claystones
Evaporites with claystones
Anhydrites

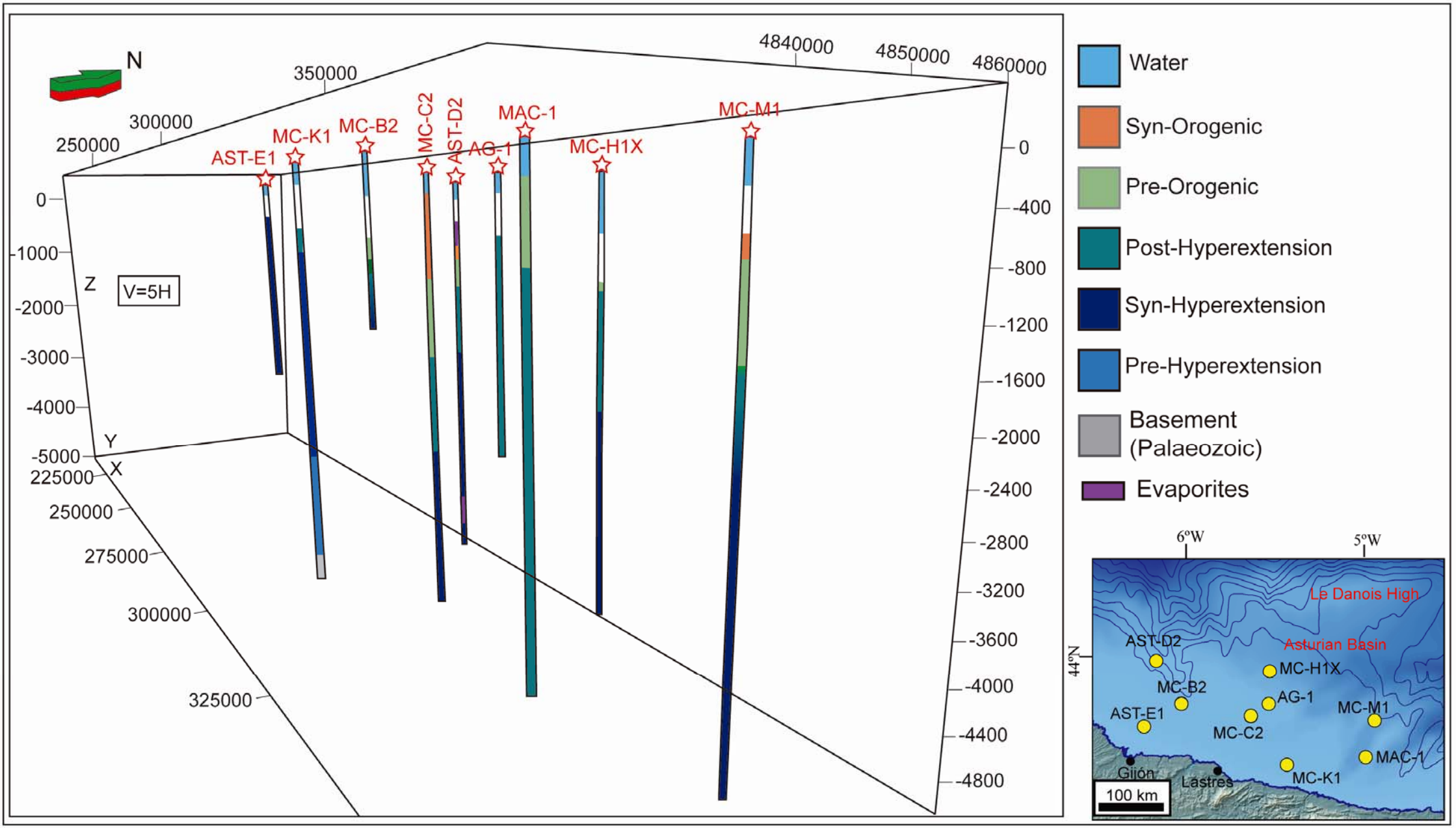
N
350000
300000
250000
4840000
4850000
4860000
AST-E1
MC-K1
MC-B2
MC-C2
AST-D2
AG-1
MAC-1
MC-H1X
MC-M1
0
-1000
-2000
-3000
-4000
-5000
Z
V=5H
Y
X
225000
250000
275000
300000
325000
0
-400
-800
-1200
-1600
-2000
-2400
-2800
-3200
-3600
-4000
-4400
-4800
Water
Syn-Orogenic
Pre-Orogenic
Post-Hyperextension
Syn-Hyperextension
Pre-Hyperextension
Basement
(Palaeozoic)
Evaporites
6ºW
5ºW
44ºN
Le Danois High
Asturian Basin
AST-D2
MC-H1X
MC-B2
AG-1
MC-M1
AST-E1
MC-C2
MAC-1
Gijón
Lastres
MC-K1
100 km

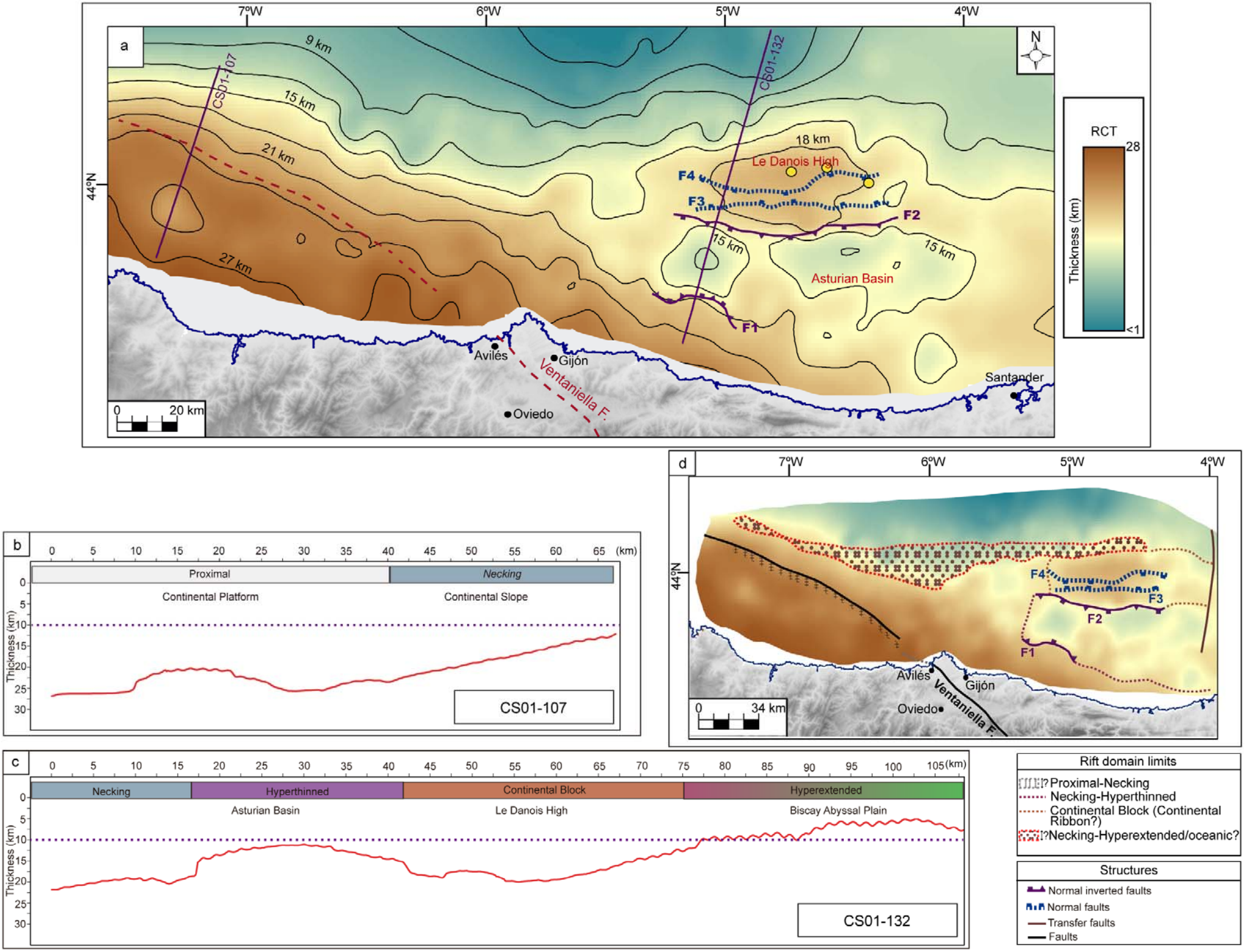
a
7ºW
6ºW
5ºW
4ºW
44ºN
N
9 km
15 km
21 km
27 km
18 km
CS01-107
CS01-132
Le Danois High
F4
F3
F2
F1
15 km
15 km
Asturian Basin
RCT
28
<1
Thickness (km)
Avilés
Gijón
Oviedo
Ventaniella F.
Santander
0
20 km
b
0 5 10 15 20 25 30 35 40 45 50 55 60 65 (km)
Proximal
Necking
Continental Platform
Continental Slope
Thickness (km)
CS01-107
c
0 5 10 15 20 25 30 35 40 45 50 55 60 65 70 75 80 85 90 95 100 105(km)
Necking
Hyperthinned
Continental Block
Hyperextended
Asturian Basin
Le Danois High
Biscay Abyssal Plain
Thickness (km)
CS01-132
d
7ºW
6ºW
5ºW
4ºW
44ºN
F4
F3
F2
F1
Avilés
Gijón
Oviedo
Ventaniella F.
0
34 km
Rift domain limits
I? Proximal-Necking
Necking-Hyperthinned
Continental Block (Continental Ribbon?)
I?Necking-Hyperextended/oceanic?
Structures
Normal inverted faults
Normal faults
Transfer faults
Faults

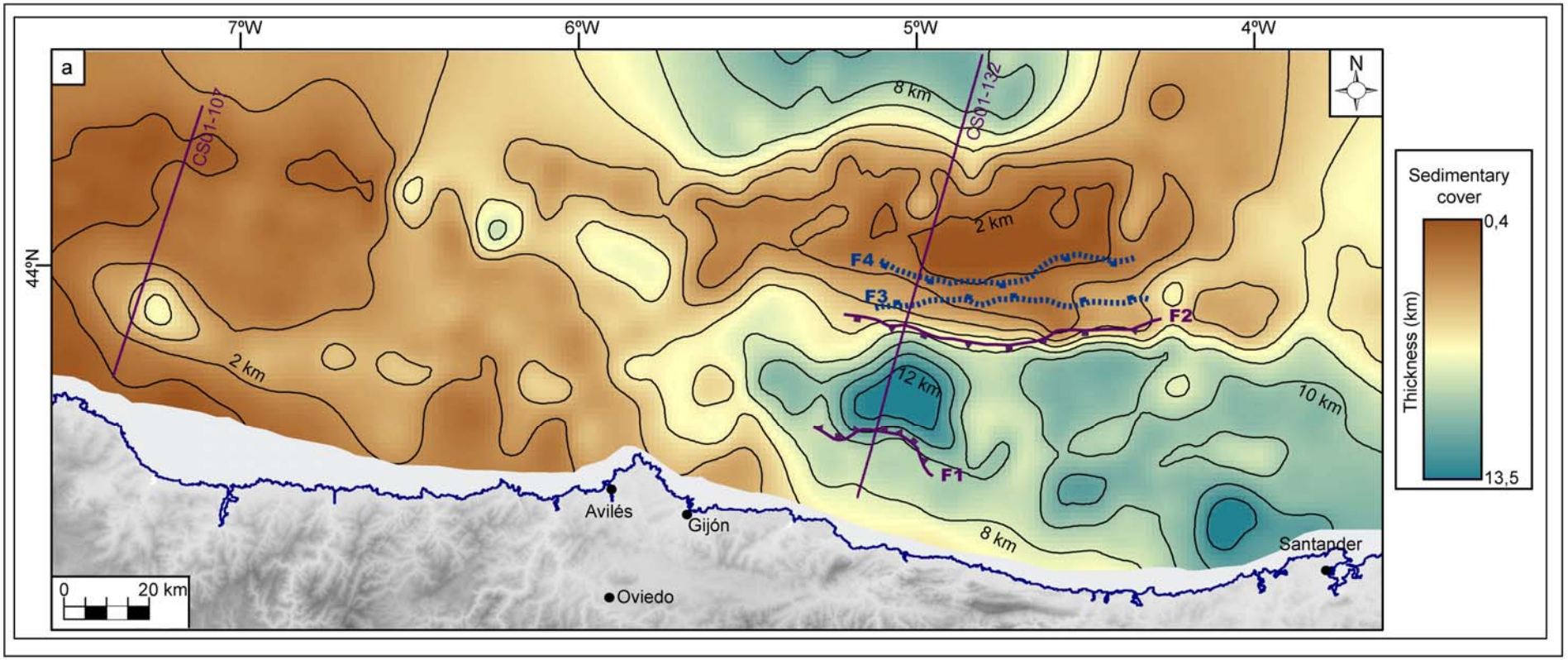
a
7ºW
6ºW
5ºW
4ºW
44ºN
N
CSO1-107
CSO1-132
8 km
2 km
F4
F3
F2
F1
12 km
10 km
2 km
8 km
Avilés
Gijón
Oviedo
Santander
0
20 km
Sedimentary cover
0,4
Thickness (km)
13,5

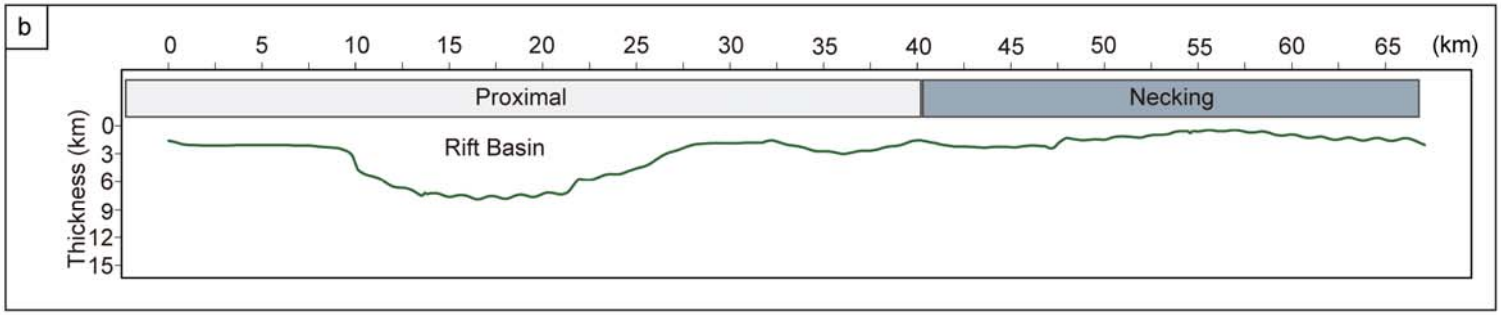
b
0 5 10 15 20 25 30 35 40 45 50 55 60 65 (km)
Proximal
Necking
Rift Basin
Thickness (km)
0
3
6
9
12
15

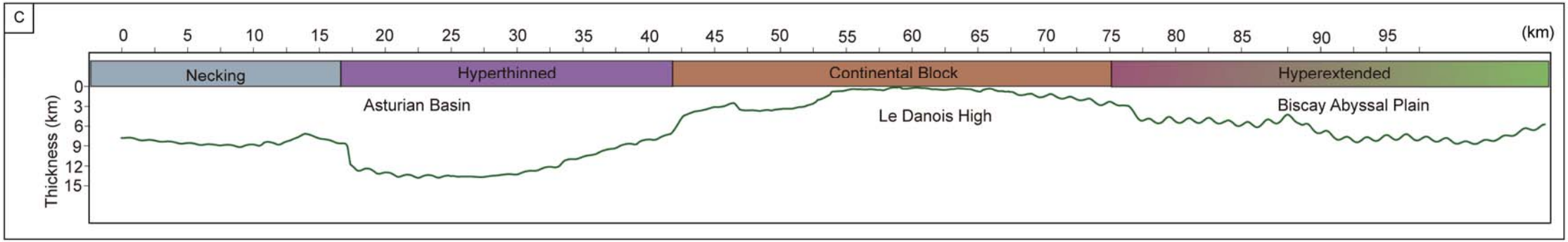
c
0 5 10 15 20 25 30 35 40 45 50 55 60 65 70 75 80 85 90 95 (km)
Necking
Hyperthinned
Continental Block
Hyperextended
Asturian Basin
Le Danois High
Biscay Abyssal Plain
Thickness (km)
0
3
6
9
12
15

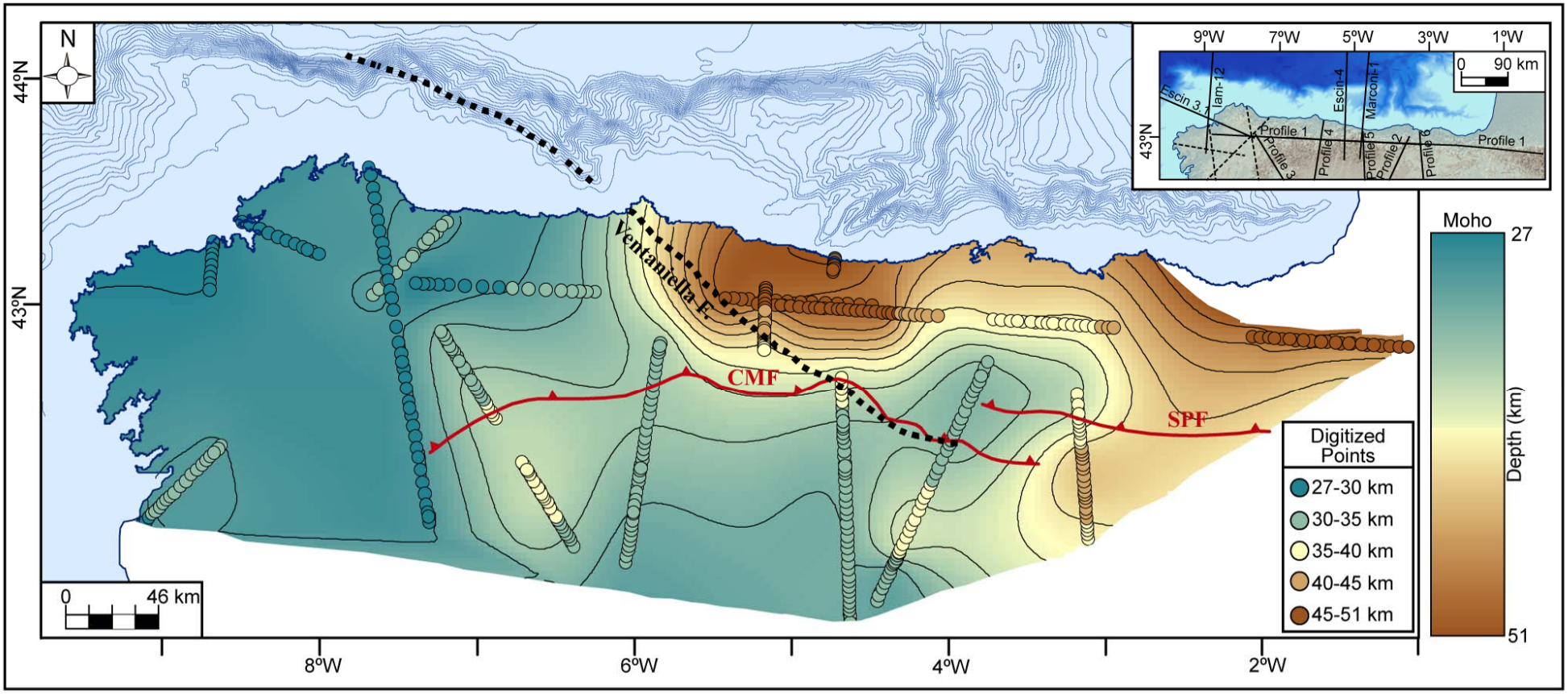
N
44ºN
43ºN
8ºW
6ºW
4ºW
2ºW
0
46 km
Ventaniella F.
CMF
SPF
9ºW
7ºW
5ºW
3ºW
1ºW
0
90 km
Escin 3
Iam-12
Escin-4
Marconi-1
Profile 1
Profile 4
Profile 5
Profile 2
Profile 3
Profile 6
Profile 1
Digitized Points
27-30 km
30-35 km
35-40 km
40-45 km
45-51 km
Moho
27
Depth (km)
51

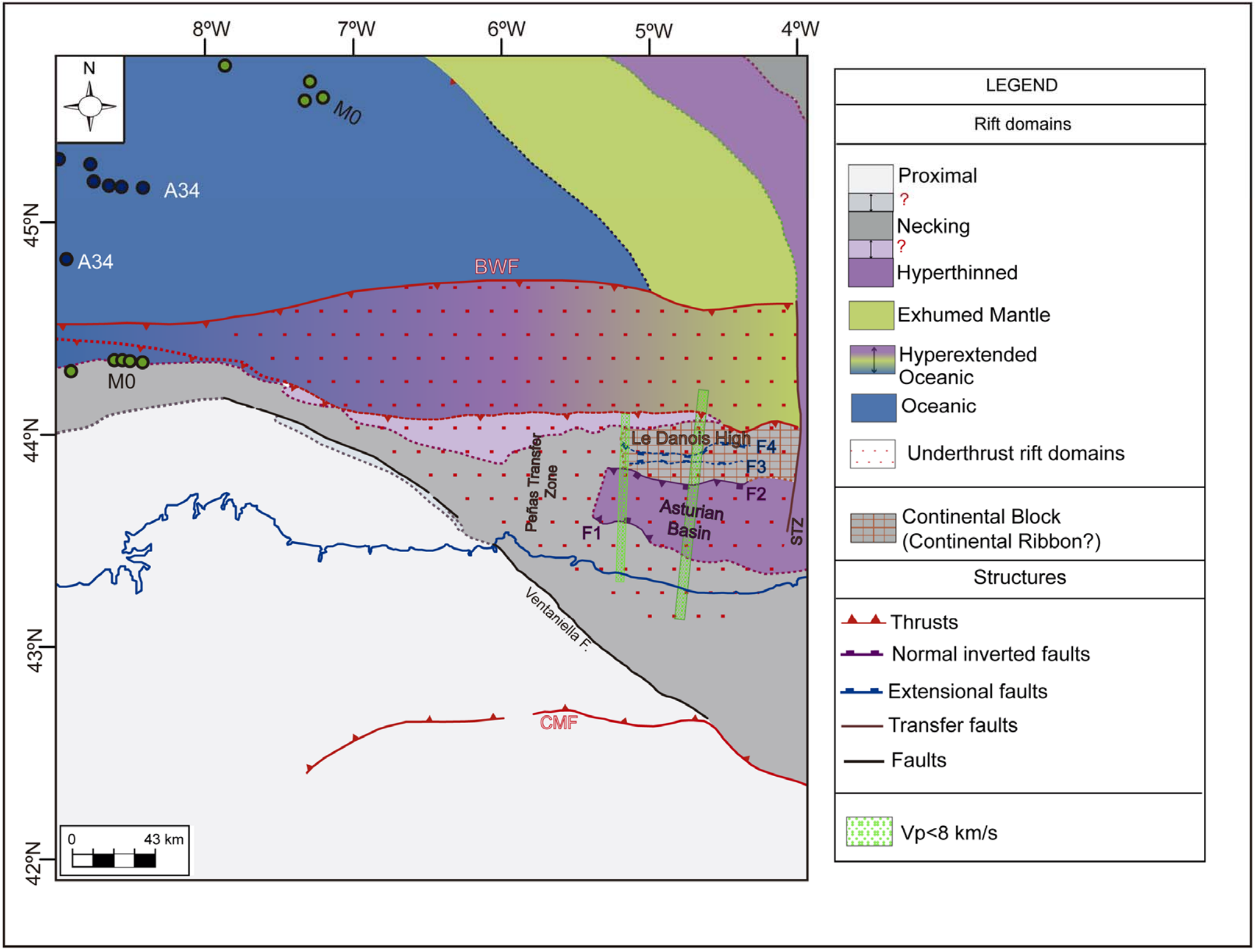
8°W
7°W
6°W
5°W
4°W
45°N
44°N
43°N
42°N
N
M0
A34
A34
BWF
M0
Le Danois High
F4
F3
F2
F1
Peñas Transfer Zone
Asturian Basin
STZ
Ventaniella F.
CMF
0
43 km
LEGEND
Rift domains
Proximal
?
Necking
?
Hyperthinned
Exhumed Mantle
Hyperextended Oceanic
Oceanic
Underthrust rift domains
Continental Block (Continental Ribbon?)
Structures
Thrusts
Normal inverted faults
Extensional faults
Transfer faults
Faults
Vp<8 km/s

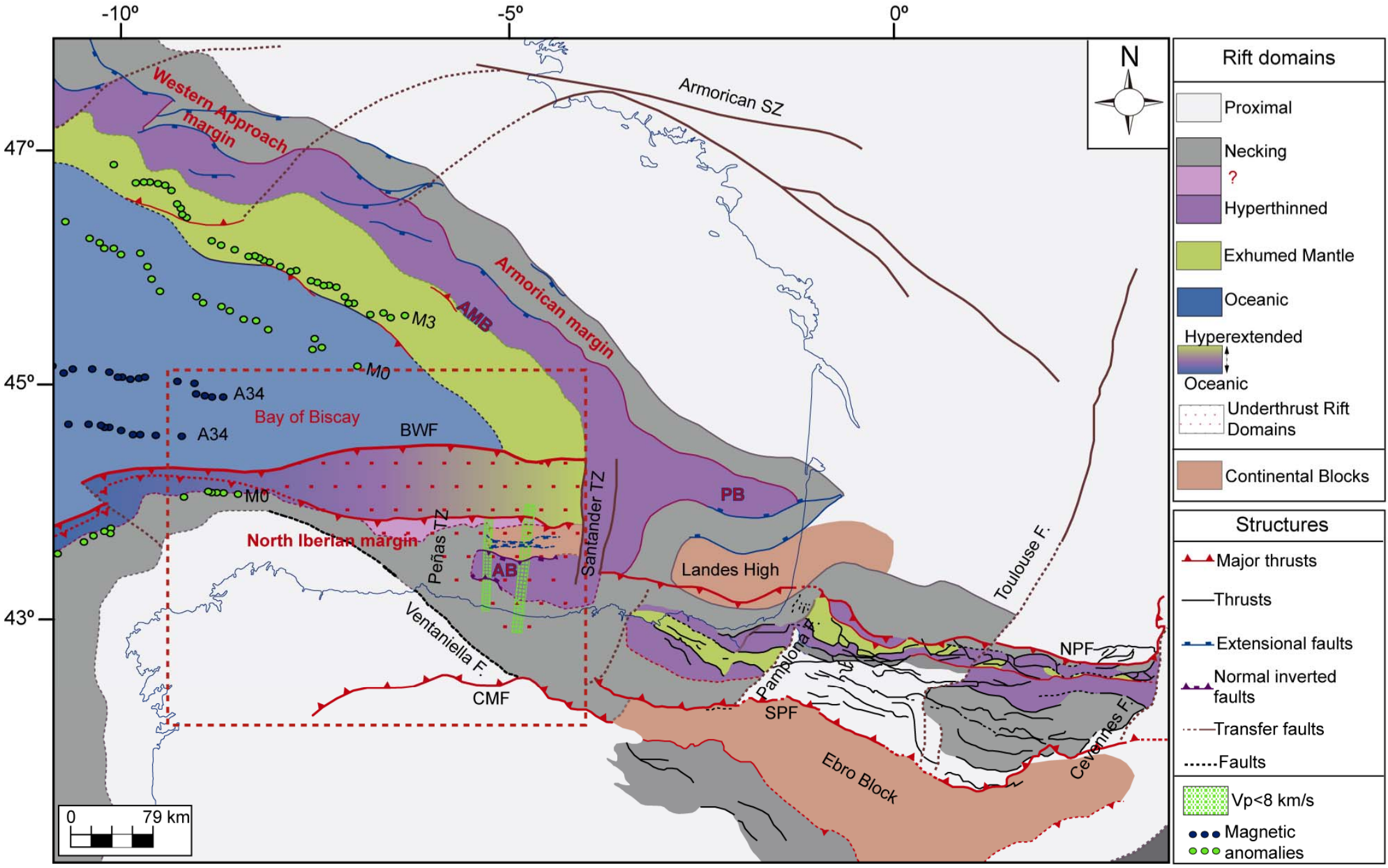
-10º
-5º
0º
47º
45º
43º
N
Western Approach margin
Armorican SZ
Armorican margin
AMB
M3
M0
A34
A34
Bay of Biscay
BWF
M0
North Iberian margin
Peñas TZ
AB
Sanfander TZ
PB
Landes High
Toulouse F.
Ventaniella F.
CMF
Pamplona F.
SPF
NPF
Cevennes F.
Ebro Block
0
79 km
Rift domains
Proximal
Necking
?
Hyperthinned
Exhumed Mantle
Oceanic
Hyperextended
Oceanic
Underthrust Rift Domains
Continental Blocks
Structures
Major thrusts
Thrusts
Extensional faults
Normal inverted faults
Transfer faults
Faults
Vp<8 km/s
Magnetic anomalies

[Tectonics]

Supporting Information for

[Constraints imposed by rift inheritance on the compressional reactivation of a hyperextended margin: mapping rift domains in the North Iberian margin and in the Cantabrian Mountains, exactly following journal article]

[P.Cadenas, G. Fernández-Viejo, J.A. Pulgar, J. Tugend, G. Manatschal & T.A. Minshull]

[(1): Department of Geology, University of Oviedo, Oviedo, Spain; (2): Institut du Physique du Globe de Strasbourg; UMR 7516, Université de Strasbourg/EOST, CNRS Strasbourg, France; (3): Ocean and Earth Science, National Oceanography Centre Southampton, University of Southampton, Southampton, United Kingdom]

Contents of this file

Introduction

This supporting file provides the uninterpreted version of the 2D seismic reflection profiles displayed in figures 3 (Figure S1) and 5 (Figure S2). As enquired by both reviewers, we provided the original seismic profiles. These profiles belong to the 2D CS01 reflection dataset, which was acquired by TGS-Nopec in 2001. Table S1 summarizes the acquisition parameters and Table S2 provides the processing parameters. We purchased the data through the ATH (http:// geoportal.minetur.gob.es/ATHvz/) as time migrated stacks. In this supporting file, we include as well an enlargement of figure 7 (Figure S3).

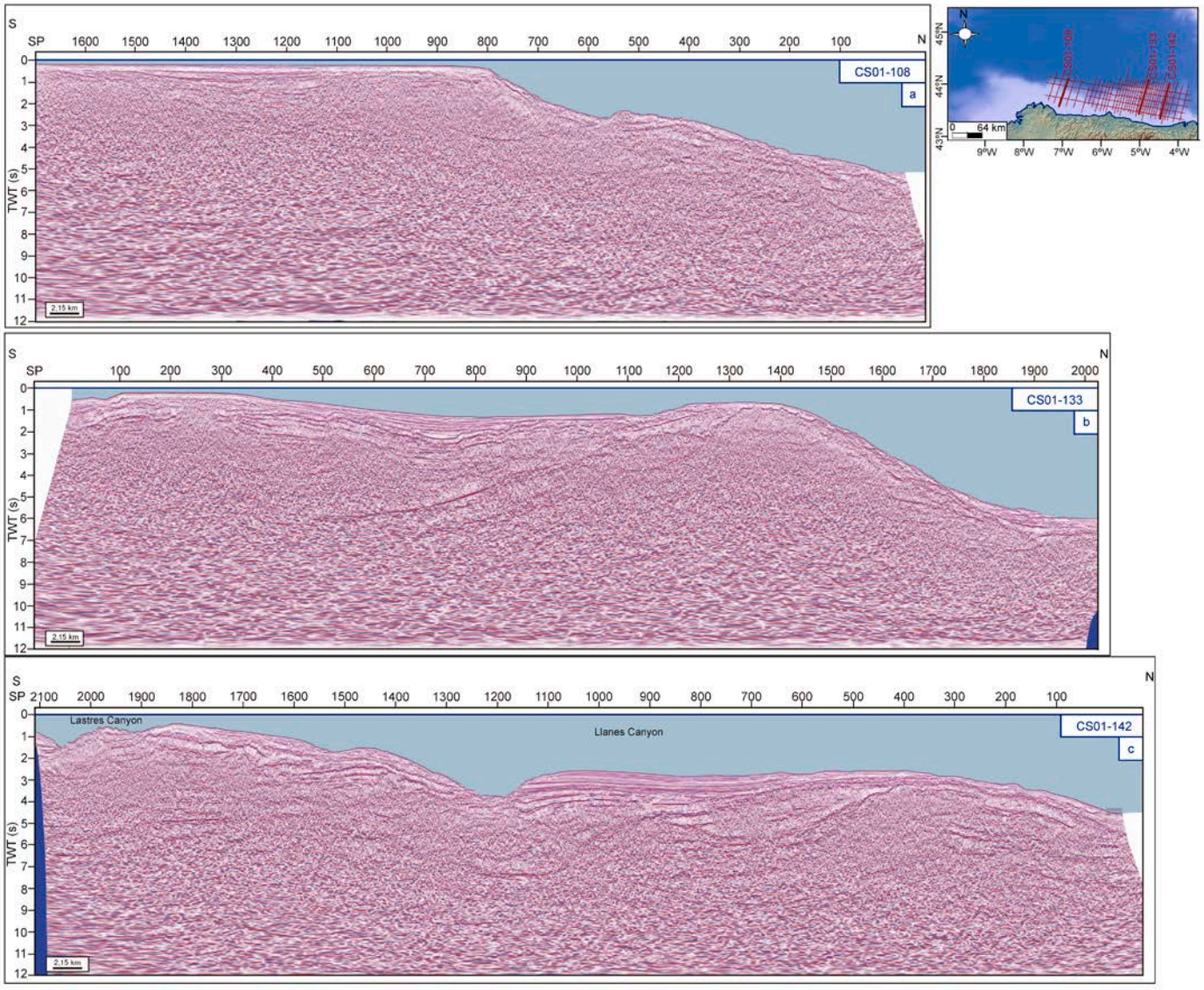
S
SP 1600 1500 1400 1300 1200 1100 1000 900 800 700 600 500 400 300 200 100
N
TWT (s)
CS01-108
a
2.15 km
S
SP 100 200 300 400 500 600 700 800 900 1000 1100 1200 1300 1400 1500 1600 1700 1800 1900 2000
N
TWT (s)
CS01-133
b
2.15 km
S
SP 2100 2000 1900 1800 1700 1600 1500 1400 1300 1200 1100 1000 900 800 700 600 500 400 300 200 100
N
Lastres Canyon
Llanes Canyon
TWT (s)
CS01-142
c
2.15 km
N
45°N
44°N
43°N
0 64 km
9°W 8°W 7°W 6°W 5°W 4°W
CS01-108
CS01-133
CS01-142

Figure S1. Representative time migrated seismic reflection profiles crossing the North Iberian margin at three different longitudes. A) CS01-108 seismic line at the westernmost area; B) CS01-133 section at the central part of the margin; C) CS01-142 seismic line located in the easternmost part of the studied zone. The inset shows the location of the reflection profiles within the seismic dataset.

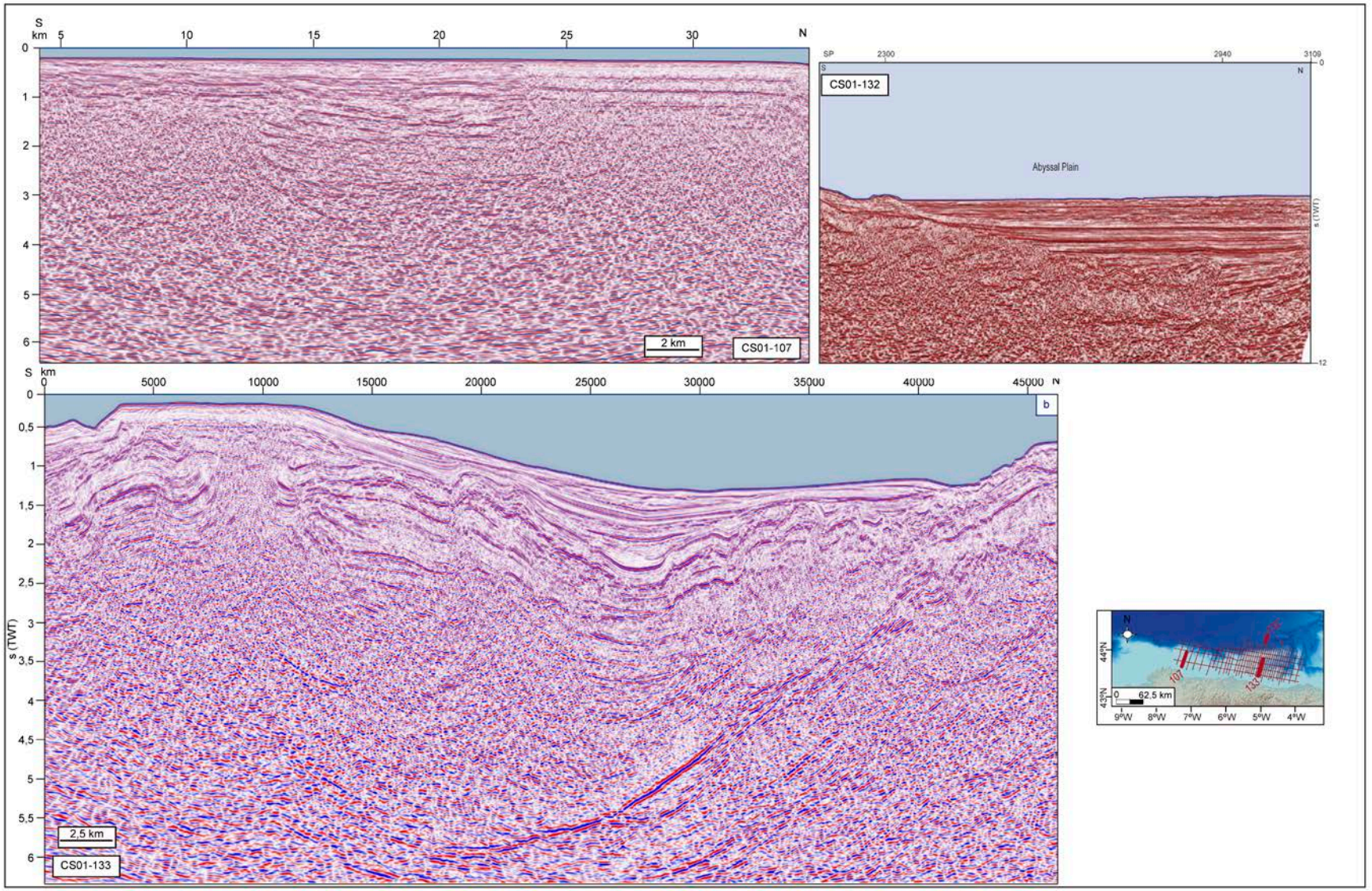
S
km
5
10
15
20
25
30
N
2 km
CS01-107
SP
2300
2940
3109
S
N
CS01-132
Abyssal Plain
s (TWT)
km
5000
10000
15000
20000
25000
30000
35000
40000
45000
b
2,5 km
CS01-133
44°N
43°N
62,5 km
9°W
8°W
7°W
6°W
5°W
4°W

Figure S2. Enlargements of three seismic reflection profiles showing the tectono-stratigraphic architecture of the main structural areas identified in the central and western North Iberian margin. Exaggerated vertical scale. A) Line CS01-107, displaying the structure of the rift basin identified in the westernmost continental platform; B) Profile CS01-133, showing the structure of the Asturian Basin in the continental platform of the central North Iberian margin; C) Profile CS01-132, in the central North Iberian margin, showing the structure of the accretionary wedge developed in the abyssal plain.

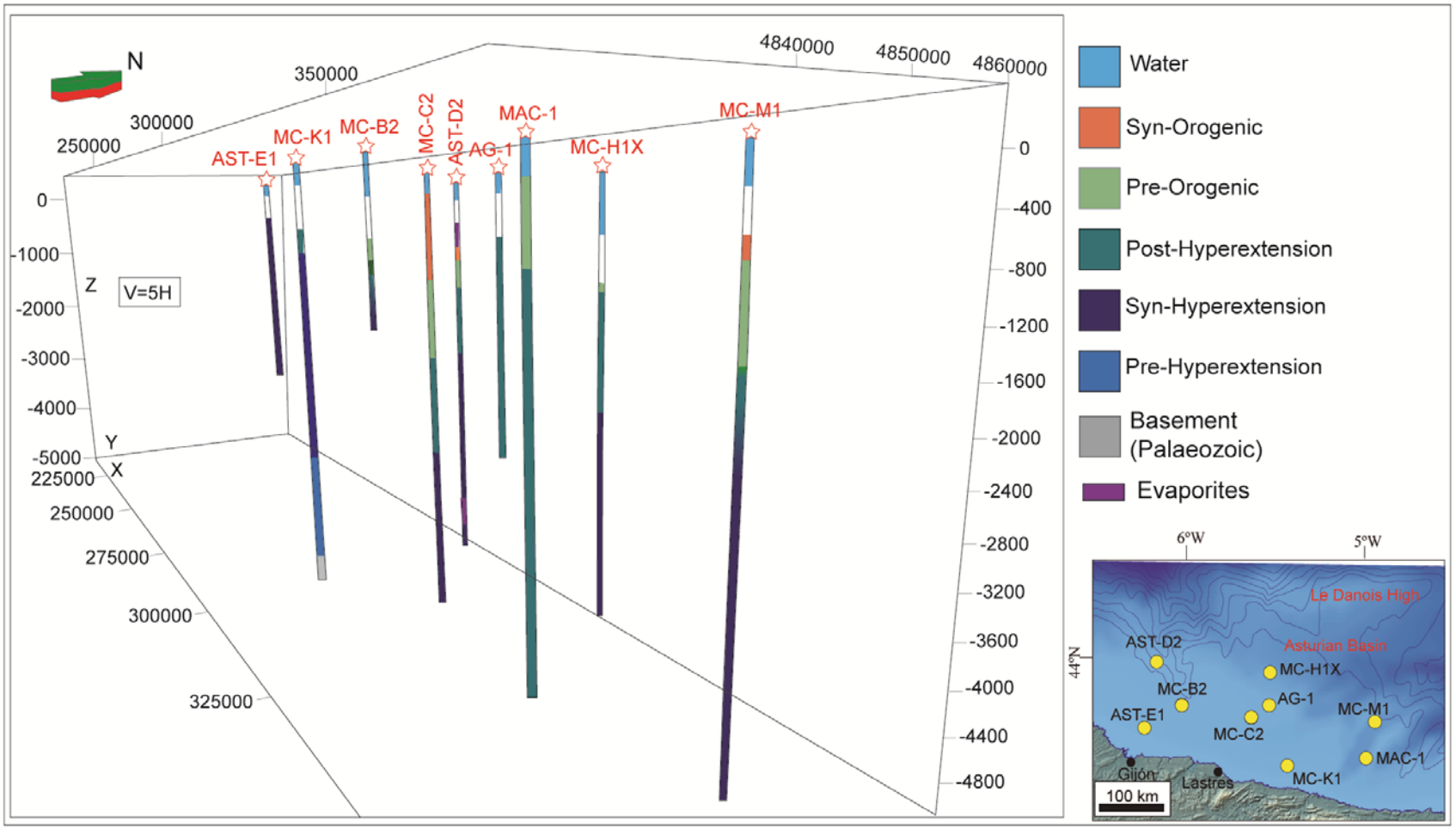

Figure S3. 3D view of nine representative boreholes drilled in the Asturian Basin showing thickness variations of the main tectono-stratigraphic units along the whole area. The original stratigraphic information has been taken from the well reports. See *Lanaja* (1987), *Gutiérrez-Claverol*

& *Gallastegui* (2002) and *Cadenas & Fernández-Viejo* (2017) for stratigraphic columns. We defined the main seismo-stratigraphic units displayed along the boreholes based on seismic to well ties.

Acquisiton parameters	
Acquisition date	September-October 2001
Vessel	M/V Nanhai 502
Survey lenght	4080 km
Number of lines	43
Recording instrument	Syntrak 480 MRS
Source type	Sleeve gun
Source volume	3680 Cu.in.
Gun depth	7 m
Shotpoint Interval	37.5 m
Group interval	25 m
Recording channles	240
Streamer depth	9m
Streamer length	6000 m
Record length	12 s
Sample interval	2 ms
Nominal fold	80

Table S1. Acquisition parameters of the CS01 seismic reflection profiles (TGS-Nopec, Acquisition report).

Input, Seg-D to Promax internal format.

Timing correction, -128 ms applied.

Filter, Zero-phase Butterworth 3-90 HZ: 18-72 dB/oct.

Resample to 4 ms, trace drop and 2D marine geometry assignment.

Datum statics, Correction to MLS.

Trace Edit and spike editor.

Minimum phase conversion, using far field source signature.

Amplitude recovery, 10dB/sec WB to 4000 ms.

Shot domain mix. 0,1.0.3,1, 0.3, 0.1, trace weighted mixing with NMO wrap.

Radon filter, NMO (1480 m/s) parabolic radon transform, modelled multiple between 300-500 ms.

NMO, Using 3 km velocity field.

Filter. Butterworth 4.2-90 HZ. 18-72dB/oct.

CDP mix, 0.7, 1,0.7 trace weighted mix with AGC wrap.

Wiener Levinson filter, Offset planes, 10-tr-pt, full application at WB+2000m, 600 ms taper.

Dip moveout correction, F-K common offset DMO 50m offset bins.

Stolt F-K migration, Smother 3 km velocities clipped at 7000 m/s.

Inverse normal move out correction, Using 3 km velocity field.

NMO analysis, Every 1.5 km.

Radon filter, Parabolic radon transform, modelled multiple muted between 100-1000 ms moveout.

Deconvolution, 3 gates, operators 120, 160, 240, gaps 24, 36 48, 11 tr average.

Remove amplitude recovery 10dB7sec WB to 4000 ms.

NMO correction, Using 1.5 km velocity field.

Amplitude recovery, scaling, offset weighting, 1/tv2 time term pre-NMO, Agc 1000ms scalars.

Muting and CDP mean stack with gain, SQRT recovery scaling applied.

Inverse Stolt F-K migration, Velocities as forward migration.

Kirchhoff Migration, Time: vel% 0 ms 100% 4000 ms.

Spectral shaping, time variant filtering, time variant scaling.

Deliverable time migration.

Table S2. Processing parameters of the CS01 seismic reflection profiles (TGS-Nopec, Acquisition report).